IRS-enhanced Integrated Sensing, Communication, and Powering Systems: Beamforming and Reflecting Optimization

Sun Mao, Lei Liu, Zhujun Yao, Mianxiong Dong, Mohammed Atiquzzaman, Schahram Dustdar, Kun Yang, and Chau Yuen

***Abstract*—This article investigates a joint optimization framework for intelligent reflecting surface (IRS)-enhanced integrated sensing, communication, and powering systems. In this framework, the base station transmits signals for simultaneous radar sensing, as well as multi-user information and power transmissions. We aim at maximizing the minimum harvested power among all users, while satisfying beampattern gain requirements for multi-target sensing and signal-to-interference-plus-noise constraints of users. To tackle this strictly non-convex problem, we employ the block coordinate descent technique to iteratively optimize the transmit beamformer of the base station, the phase shift matrix of the IRS, and the power splitting ratios of users. The semi-definite relaxation method is utilized to obtain the optimal transmit beamformer of the base station, and the tightness of the rank-one relaxation is demonstrated. Furthermore, we develop a penalty function-based algorithm and use successive convex approximation techniques to determine the optimal phase shift matrix of the IRS. Additionally, closed-form expressions are derived for the optimal power splitting ratios. Moreover, by exploiting the Bernstein-type inequality, we further designed the robust beamforming and power splitting scheme for considered systems under stochastic channel estimation errors. Numerical results demonstrate that the proposed IRS-enhanced method outperforms several benchmark methods in terms of the minimum harvested power among all users.**

***Index Terms*—6G, intelligent reflecting surface, wireless power transfer, integrated sensing and communication networks.**

I. Introduction

The sixth generation (6G) mobile communication networks expect to empower a variety of innovative applications including autonomous driving, industrial automation, smart cities, and so forth. To improve the service quality for such environment-aware applications, integrated sensing and communication (ISAC) is regarded as a core technology [1]–[4]. In ISAC, the resources of radar sensing and wireless communications can be shared to improve the hardware reuse, energy and spectral efficiency [5]–[8]. Meanwhile, it is of great importance to prolong the lifetime of wireless devices in an efficient and low-cost manner. The prospect of introducing wireless power transfer (WPT) into ISAC systems has great potential to realize this target, and it will create a new paradigm, i.e., integrated sensing, communication, and powering systems. Nevertheless, the performance of such an integrated system is fundamentally restricted by the severe path-loss of WPT, and the severe co-channel interference between radar sensing and information transmissions [9]–[14].

With the rapid advancement of information metamaterials, IRS is regarded as an innovative technology to reconstruct wireless propagation environments [15]–[19]. Generally, an IRS comprises numerous passive or active reflection units that can adjust the amplitude and phase of incident signals. This refined reflect beamforming improves signal strength at intended receivers while reducing harmful co-channel interference. Additionally, deploying and configuring multiple IRSs provides extra communication links to enhance network coverage. Inspired by these advantages, IRS holds great potential for improving the performance of integrated sensing, communication, and powering systems. In [20]–[25], IRS was utilized to improve diverse performance metrics (such as sum rate, total harvested power, maximum transmit power, etc.) for simultaneous wireless information and power transfer (SWIPT) systems. Aforementioned literature considered conventional linear power harvesting model, which cannot reflect the non-linearity of practical power harvesters. To this end, the literature in [26]–[29] investigated the beamforming method for IRS-enhanced SWIPT systems taking into account of non-linear power harvesting model.

Furthermore, IRS was also exploited to enhance the ISAC performance [30]–[35]. In [36]–[39], the authors focused on optimizing the communication performance for IRS-aided ISAC systems, while satisfying the sensing requirements. In [40], Luan *et al.* aimed at maximizing the sensing mutual information through optimizing transmit and reflect beamformers. In [41], Liu *et al.* developed the joint waveform and beamforming optimization method to maximize the radar output signal-to-interference-plus-noise (SINR), while guaranteeing the communication requirements. Tong *et al.* in [42] further revealed the maximum radar SINR for multi-IRS-aided ISAC systems in clutter environments. In [43], Song *et al.* utilized the IRS to achieve non-line-of-sight radar sensing. Moreover, they revealed the cramér-rao lower bound for estimation error in the scenarios with point targets and extended targets. In [44], [45], active IRS was adopted to tackle the path

S. Mao, Z. J. Yao and C. Yuen are with the School of Electrical and Electronic Engineering, Nanyang Technological University, 639798, Singapore (e-mails: eee-sun.mao@ntu.edu.sg; eee-zjyao@ntu.edu.sg; chau.yuen@ntu.edu.sg).

L. Liu is with the State Key Laboratory of Integrated Service Networks, Xidian University, Xi'an 710071, China. (e-mail: tianjiaoliulei@163.com).

M. X. Dong is with the Department of Sciences and Informatics, Muroran Institute of Technology, Muroran 050-8585, Japan (e-mail: mx.dong@csse.muroran-it.ac.jp).

M. Atiquzzaman is with the School of Computer Science, University of Oklahoma, Norman, OK 73019 USA (e-mail: atiq@ou.edu).

S. Dustdar is with TU Wien, 1040 Vienna, Austria. (e-mail: dustdar@infosys.tuwien.ac.at).

K. Yang is with the School of Computer Science and Electronic Engineering, University of Essex, Colchester CO4 3SQ, U.K. (e-mail: kunyang@essex.ac.uk).

attenuation in ISAC systems. Moreover, Wang *et al.* in [46] utilized the simultaneous transmitting and reflecting surface to improve the coverage of ISAC systems. Double-IRS was exploited to improve the efficiency and coverage of ISAC in [47]. In summary, Table I illustrates the difference between this article and existing literature.

As shown in Table I, the authors in [20]–[29] investigated joint transmit/reflect beamforming and power splitting strategies for IRS-aided SWIPT systems. Besides, [34]–[47] aimed at utilizing the IRS to enhance the ISAC performance. Nevertheless, existing literature ignored the optimal design for IRS-aided integrated sensing, communication, and powering systems, which is essential to meet the diverse service requirements in 6G era. Noted that this research problem is extremely difficult due to the complex coupled relationship among radar sensing, communication, and powering. As expected, the radar sensing can cause harmful co-channel interference to information transmission, but the extra sensing signals become beneficial to power harvesting. In addition, information transmission and power harvesting move toward perfect opposition in SWIPT, i.e., if the wireless device splits a larger ratio of received signals to decode information, it will inevitably result in the reduction of harvested power level. While IRS offers substantial performance gains, configuring it effectively to optimize the performance of such an integrated system presents significant challenges. Therefore, how to develop the optimal transmission and reflection optimization strategies for IRS-aided integrated sensing, communication, and powering systems for balancing the performance of radar sensing, communication, and powering is an important but difficult problem. Such observation motivates our study in this article.

This article considers a typical IRS-assisted integrated sensing, communication, and powering system, where the base station (BS) transmits signals for conducting wireless power and information transmissions to multiple users, and multi-target radar sensing simultaneously. The contribution of this article is outlined as follows.

- To achieve performance tradeoff between radar sensing, information, and power transfer, this paper formulates a minimum harvested power maximization problem, under the constraints of minimum sensing beampattern gains for multiple targets, minimum SINR requirements of users, and maximum transmit power of BS.
- To address the formulated non-convex problem, we propose a block coordinate descent-based approach to alternately optimize the transmit beamformer at the BS, the phase shift matrix of the IRS, and the power splitting ratios of users. Specifically, we employ the semi-definite relaxation technique to obtain the optimal transmit beamformer at the BS, and derive the closed-form expression of rank-one transmit beamforming. Furthermore, we design a penalty function-based method to determine the optimal phase shift matrix of the IRS. Besides, we obtain a closed-form solution for the optimal power splitting ratio. Meanwhile, we reveal the proposed alternating optimization method is ensured to converge within polynomial time.
- To tackle the unavoidable channel estimation errors, we further investigate a robust transmit/reflect beamforming and power splitting optimization framework for the considered system under stochastic CSI uncertainties. In particular, the Bernstein-type inequality is utilized to transform the semi-infinite SINR and power harvesting constraints—arising from imperfect CSI—into deterministic and tractable forms. Furthermore, an alternating optimization strategy, in conjunction with variable substitution and a penalty function-based algorithm, is employed to jointly design the robust transmit/reflect beamforming and power splitting scheme.
- Simulation results show that our proposed method achieves significantly higher harvested power compared to the benchmark scheme without optimal IRS configuration. Additionally, we show that radar sensing inevitably leads to a performance reduction in SWIPT, and our proposed method performs closely to the benchmark method without radar sensing when the sensing beampattern gain requirement is sufficiently small. Meanwhile, we also verify that the proposed method outperforms the sum harvested power maximization-based method, especially when the SINR threshold is small.

The structure of this article is outlined as follows. Section II presents the system model and formulates the optimization problem for IRS-assisted integrated sensing, communication, and powering systems. Section III details the development of an optimization algorithm designed for joint transmit beamforming, reflection coefficient matrix configuration, and power splitting ratio determination. Section IV extends the formulated problem to the scenario with channel estimation errors. Section V provides extensive numerical results, demonstrating the performance gains achieved by the proposed approach. Finally, Section VI concludes the article with a summary of findings.

Symbol Notations: The notation $(\cdot)^T$, $(\cdot)^H$, $\mathrm{Tr}(\cdot)$, $\mathrm{Vec}(\cdot)$, $\mathrm{diag}(\cdot)$, and $\mathrm{Rank}(\cdot)$ denote the transpose, conjugate transpose, trace, matrix vectorization, diagonalization, and rank operations, respectively. $|\cdot|$ and $\|\cdot\|$ represent the absolute value of a complex number and the norm of a complex vector, respectively. $\otimes$ indicates the Kronecker product. Additionally, $\mathcal{O}(\cdot)$ is used to denote the computational complexity of an algorithm.

II. System Model and Problem Formulation

As depicted in Fig. 1, this article focuses on an IRS-enhanced integrated sensing, communication, and powering system including a multi-functional BS installed with M antennas, K single-antenna users, an IRS with N reflec-

TABLE I: Synopsis of related works

Ref.	Optimization goal	IRS	Sensing	Communication	WET
[20]	Sum rate	✓	✗	✓	Linear model
[21]	Weighted total harvested power	✓	✗	✓	Linear model
[22]	Sum rate &total harvested power	✓	✗	✓	Linear model
[23]	Weighted sum rate & Weighted total harvested power	✓	✗	✓	Linear model
[24]	Minimum achievable rate of all users	✓	✗	✓	Linear model
[25], [26]	Total transmit power	✓	✗	✓	Linear/Non-linear model
[27]	Rate-energy region	✓	✗	✓	Non-linear model
[28], [29]	Energy efficiency	✓	✗	✓	Non-linear model
[34]	Total transmit power	✓	✓	✓	✗
[35]	Total energy consumption	✓	✓	✓	✗
[36]	Communication SINR	✓	✓	✓	✗
[37], [38]	Sum rate	✓	✓	✓	✗
[39]	Sum rate &Weighted sensing mutual information	✓	✓	✓	✗
[40]	Sensing mutual information	✓	✓	✓	✗
[41]	Radar output SINR	✓	✓	✓	✗
[42]	Radar &communication SINR	✓	✓	✓	✗
[43]	Cramér-rao lower bound	✓	✓	✓	✗
[44]	Beampattern error	✓	✓	✓	✗
[45], [46]	Sensing Beampattern gain	✓	✓	✓	✗
[47]	Sensing accuracy & Spectral efficiency	✓	✓	✓	✗
This article	Minimum harvested power	✓	✓	✓	Linear &Non-linear model

tion elements, and L sensing targets[1]. The sets of users, IRS reflection elements, and sensing targets are represented by $\mathcal{K} = \{1, 2, \cdots, K\}$, $\mathcal{N} = \{1, 2, \cdots, N\}$, and $\mathcal{L} = \{1, 2 \cdots, L\}$, respectively. In the considered system, the BS performs the downlink information and power transmissions to users, and meanwhile performs the radar sensing towards L targets. Furthermore, the IRS is utilized to reconstruct wireless channels, enhancing the efficiency of wireless information and power transfer while mitigating severe co-channel interference between information and radar signals. Notably, in scenarios where the direct links between the BS and users are completely obstructed by obstacles, the IRS becomes indispensable in establishing reflection links to facilitate downlink power and information transmission. This work considers a general scenario encompassing both direct and reflection links, with the proposed method also applicable to cases where direct links are absent. For reference, the symbols of this article are outlined in Table II.

To facilitate radar sensing, information, and power transfer, it is assumed that the BS transmits information signals $\{s_k\}_{k=1}^K$ to K users, alongside a dedicated radar signal

[1]Given the inherent high path loss characteristic of radio frequency-based wireless power transfer, the proposed system demonstrates particular suitability for deployment in application scenarios with limited coverage areas, including smart factories, warehouses, airplanes, etc. To exemplify, consider a smart warehouse as a representative use case, the system architecture consists of a multi-functional BS installed at a central or elevated location, an IRS mounted on walls or ceilings, a set of low-power devices such as environmental sensors, RFID tags, etc., as well as multiple sensing targets corresponding to critical zones or moving entities within the warehouse. In this context, the BS simultaneously performs downlink information and power transfer to low-power devices through IRS-assisted beamforming, while concurrently performing target sensing operations. This integrated design enables intelligent monitoring and real-time situational awareness, thereby laying a solid foundation for the realization of automated and smart warehouse management systems.

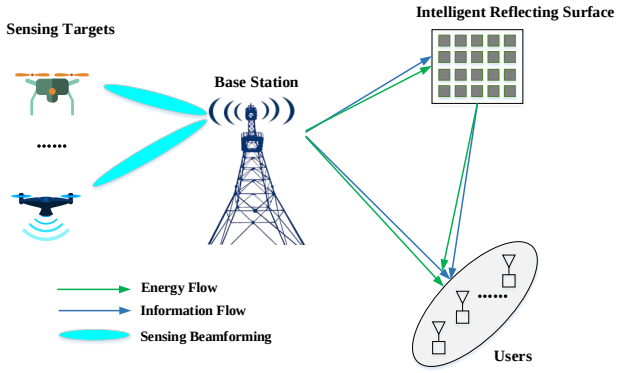

Fig. 1: IRS-enhanced integrated sensing, communication, and powering systems.

TABLE II: Summary of major symbols

Notation	Description
K	Number of users
L	Number of sensing targets
N	Number of reflection units at IRS
M	Number of antennas at BS
P_B	Transmission power of BS
δ_k^2/ζ_k^2	Gaussian noise power at k-th user
θ_n	Phase shift of n-th reflection unit at IRS
η_k	Linear power conversion efficiency at k-th user
E_k	Power harvested by k-th user
ϕ_l	Sensing direction toward l-th target
d	Distance between adjacent antennas at BS
λ	Carrier wavelength
$P_{\max,B}$	Maximum transmission power of BS
$\gamma_{\min,k}$	Minimum SINR requirement of k-th user
$b_{\min,l}$	Minimum beampattern gain requirement toward k-th target

$\mathbf{x}_0 \in \mathbb{C}^{M\times 1}$.The information signals $\{s_k\}_{k=1}^K$ are modeled as independent random variables with zero mean and unit variance. The radar signal $\mathbf{x}_0$ is assumed to have zero mean and a covariance matrix $\mathbf{S}_0 = \mathbb{E}(\mathbf{x}_0\mathbf{x}_0^H) \succeq 0$. Let $\mathbf{w}_k \in \mathbb{C}^{M\times 1}$ represent the transmit beamformer associated with s_k. Accordingly, the downlink transmitted signal at the BS can be expressed as

$$\mathbf{x} = \mathbf{x}_0 + \sum_{k=1}^{K} \mathbf{w}_k s_k. \tag{1}$$

Unlike conventional single-beam information transmission, this work considers a general multi-beam transmission scheme for the radar signal $\mathbf{x}_0$. Specifically, the radar signal is expressed as $\mathbf{x}_0 = \sum_{l=1}^{M} \mathbf{t}_{r,l} s_{r,l}$, where $s_{r,l}$ and $\mathbf{t}_{r,l}$ represent the l-th radar waveform and its corresponding transmit beamformer, respectively. The radar waveforms $\{s_{r,l}\}$ are independent pseudorandom sequences with zero mean and unit variance. The radar beamforming vectors $\{\mathbf{t}_{r,l}\}_{l=1}^M$ are derived through the eigenvalue decomposition of the covariance matrix $\mathbf{S}_0$ [48]. Moreover, the total transmit power at the BS is expressed as

$$\begin{aligned} P_B &= \mathbb{E}\left(\|\mathbf{x}_0 + \sum_{k=1}^{K} \mathbf{w}_k s_k\|^2\right) \\ &= \mathrm{Tr}(\mathbf{S}_0) + \sum_{k=1}^{K} \|\mathbf{w}_k\|^2. \end{aligned} \tag{2}$$

A. IRS-assisted SWIPT for Users

Let us define $\mathbf{h}_k^H = \mathbf{h}_{r,k}^H \Gamma \mathbf{G} + \mathbf{h}_{d,k}^H$, where $\mathbf{G} \in \mathbb{C}^{N\times M}$, $\mathbf{h}_{r,k}^H \in \mathbb{C}^{1\times N}$, and $\mathbf{h}_{d,k}^H \in \mathbb{C}^{1\times M}$ represent the channels from the BS to the IRS, from the IRS to the k-th user, and directly from the BS to the k-th user, respectively. The IRS reflection matrix is defined as $\Gamma = \mathrm{diag}\{e^{j\theta_1}, e^{j\theta_2}, \cdots, e^{j\theta_N}\}$, where $\theta_n \in (0, 2\pi]$ is the phase shift applied by the n-th reflection element. Hence, the received signal at the k-th user is expressed as

$$y_k = \mathbf{h}_k^H(\mathbf{x}_0 + \sum_{k=1}^{K} \mathbf{w}_k s_k) + n_k, \forall k \in \mathcal{K}, \tag{3}$$

where $n_k \sim \mathcal{CN}(0, \delta_k^2)$ represents the additive Gaussian noise. It is important to highlight that the channel state information (CSI) of IRS-aided integrated sensing, communication, and powering systems can be estimated by adopting separate channel estimation methods with semi-passive IRS, and cascaded channel estimation methods with full-passive IRS [49]. In Section III, we assume perfect CSI to characterize the theoretical performance bounds of the proposed IRS-enhanced sensing, communication, and powering framework. Furthermore, we will further investigate the robust beamforming strategy for the considered systems under CSI estimation errors in Section IV.

Furthermore, each user adopts a power splitting architecture to balance power harvesting and information reception[2]. For the k-th user, a portion α_k of the received downlink signal is allocated for information decoding, while the remaining $1-\alpha_k$ is utilized for power harvesting[3] Therefore, the signal for information decoding at the k-th user is given by

$$y_{\text{ID,k}} = \sqrt{\alpha_k}(\mathbf{h}_k^H(\mathbf{x}_0 + \sum_{k=1}^{K} \mathbf{w}_k s_k) + n_k) + z_k, \forall k \in \mathcal{K}, \tag{4}$$

where $z_k \sim \mathcal{CN}(0, \zeta_k^2)$ indicates the additive Gaussian noise at the information decoder of k-th user. The SINR of k-th user for decoding information is written as [4]

$$\text{SINR}_k = \frac{\alpha_k |\mathbf{h}_k^H \mathbf{w}_k|^2}{\alpha_k \sum\limits_{i=1, i\neq k}^{K} |\mathbf{h}_k^H \mathbf{w}_i|^2 + \alpha_k \mathbf{h}_k^H \mathbf{S}_0 \mathbf{h}_k + \alpha_k \delta_k^2 + \zeta_k^2}, \forall k \in \mathcal{K}. \tag{5}$$

Meanwhile, the signal for power harvesting at the k-th user is given by

$$y_{\text{EH,k}} = \sqrt{1-\alpha_k}(\mathbf{h}_k^H(\mathbf{x}_0 + \sum_{k=1}^{K} \mathbf{w}_k s_k) + n_k), \forall k \in \mathcal{K}. \tag{6}$$

Denoting $\eta_k \in (0, 1]$ as the power conversion efficiency of k-th user, the power harvested by k-th user is expressed as

$$E_k = \eta_k(1-\alpha_k)(\mathbf{h}_k^H \mathbf{S}_0 \mathbf{h}_k + \sum_{i=1}^{K} |\mathbf{h}_k^H \mathbf{w}_i|^2 + \delta_k^2), \forall k \in \mathcal{K}. \tag{7}$$

B. Target Sensing

To achieve the efficient radar sensing, the beamforming scheme is designed to form the strong beampattern gain towards L targets. According to [51], the beampattern gain $\rho(\phi_l)$ towards l-th target is written by

$$\rho(\phi_l) = \mathbf{a}^H(\phi_l)\left(\mathbf{S}_0 + \sum_{k=1}^{K} \mathbf{w}_k \mathbf{w}_k^H\right)\mathbf{a}(\phi_l), \forall l \in \mathcal{L}, \tag{8}$$

[2]In comparison to time switching-based power transfer schemes, the power splitting architecture offers distinct implementation advantages. The power splitting approach can be realized using relatively simple analog components, eliminating the need for precise synchronization and rapid switching between power harvesting and information decoding modes. Furthermore, time switching-based schemes inherently suffer from spectral efficiency limitations due to their time-division operation between power and information transfer. Motivated by these considerations, our study employs the power splitting-based architecture for simultaneous wireless information and power transfer.

[3]The power splitting ratio α_k is typically determined based on the trade-off between power harvesting and information decoding. A smaller α_k is chosen to meet higher power harvesting requirements, whereas a larger α_k enhances the SINR for information reception.

[4]Notice that the sensing signal $\mathbf{x}_0$ is generally pre-determined sequences that can be known by the BS. In addition, the BS can send the radar signal $\mathbf{x}_0$ and the CSI $\{\mathbf{h}_k\}_{k=1}^K$ to users before the ISAC transmissions. During the transmissions, the k-th user can cancel $\mathbf{h}_k^H \mathbf{x}_0$ from y_k. As observed, the cancellation of radar interference signal at users will increase the signaling overheads of considered systems, and meanwhile it also reduces the amount of harvested power from downlink received signals of users. In this paper, we aim at maximizing the minimum harvested power among all users, while satisfying the information transmissions and radar sensing requirements. Therefore, we consider that the users do not need to remove the radar interference signal before decoding information and harvesting power [48], [50].

where $\mathbf{a}(\phi_l) = \frac{1}{\sqrt{M}}[1, e^{j\frac{2\pi d \sin(\phi_l)}{\lambda}}, \cdots, e^{j\frac{2\pi d(M-1)\sin(\phi_l)}{\lambda}}]^T$ represents the array steering vector of BS with direction ϕ_l, λ indicates the carrier wavelength, and d denotes the distance between two adjacent antennas. It is worth noting that this paper assumes that the target directions θ_l are perfectly known at the BS[5]. This is a common assumption in the existing literature (e.g., [48], [50]), which allows us to focus on the joint beamforming and power splitting design and to establish a performance upper bound that serves as a useful benchmark for future extensions involving imperfect angle information.

C. Problem Formulation

This work aims at maximizing the minimum harvested power among all users, while satisfying the SINR constraints of users and multi-target sensing requirements. Moreover, the transmit beamforming $\{\mathbf{w}_k, \mathbf{S}_0\}$ of BS, the phase shift matrix Γ of IRS, and power splitting ratios $\{\alpha_k\}$ of users are jointly optimized to achieve such a design goal. Such a joint optimization problem is expressed as

$$\begin{aligned} \underset{\{\mathbf{w}_k,\alpha_k,\mathbf{S}_0,\Gamma\}}{\text{maximize}} \quad & \min_{k\in\mathcal{K}} E_k \\ \text{s.t.} \quad & \text{C1: } \mathrm{Tr}(\mathbf{S}_0) + \sum_{k=1}^{K} \|\mathbf{w}_k\|^2 \le P_{\max,B}, \\ & \text{C2: } \mathrm{SINR}_k \ge \gamma_{\min,k}, \forall k \in \mathcal{K}, \\ & \text{C3: } \rho(\phi_l) \ge b_{\min,l}, \forall l \in \mathcal{L}, \\ & \text{C4: } 0 \le \theta_n \le 2\pi, \forall n \in \mathcal{N}, \\ & \text{C5: } 0 \le \alpha_k \le 1, \forall k \in \mathcal{K}, \\ & \text{C6: } \mathbf{S}_0 \succeq 0, \end{aligned} \tag{9}$$

where $P_{\max,B}$ is the maximum transmit power of BS, $\gamma_{\min,k}$ denotes the minimum SINR requirement of k-th user, and $b_{\min,l}$ specifies the minimum beampattern gain for the l-th target. In Problem (9), constraint C1 limits the BS transmit power, C2 enforces the SINR requirements for users, and C3 ensures the beampattern gain for radar sensing. Constraints C4, C5, and C6[6] correspond to the IRS phase shift configuration, power splitting ratio, and transmit beamforming design, respectively.

Remark 1: The formulated problem (9) is strictly non-convex due to the following reasons: 1) the highly coupled optimization variables at SINR_k and E_k, including transmit beamformer $\mathbf{w}_k$ and phase shift matrix Γ, the power splitting ratio α_k and the transmit beamformer $\mathbf{w}_k$, etc. 2) the non-smooth and non-concave objective function $\min_{k\in\mathcal{K}} E_k$; 3) the non-convex beampattern gain requirements.

It is important to note that conventional convex optimization techniques cannot be directly applied to address the non-convex nature of problem (9). Furthermore, heuristic algorithms, such as particle swarm optimization and greedy methods, often suffer from high computational complexity and uncertain convergence properties. To overcome these challenges, the block coordinate descent technique is first leveraged to construct an alternating optimization framework, enabling the decoupling of the optimization variables. Subsequently, advanced methods, including variable substitution, semi-definite relaxation, and a penalty-function-based approach, are employed to efficiently solve the resulting subproblems. Finally, we rigorously demonstrate that the proposed alternating optimization framework ensures convergence within polynomial time.

[5]Noted that various methods have been developed to obtain target angular information, such as wide-beam initial scanning [52], recursive estimation algorithms (e.g., Kalman filtering) [53], and sensor fusion approaches that combine RF measurements with auxiliary modalities like visual sensors, inertial measurement units (IMUs), or GPS [54].

[6]Note that $\mathbf{S}_0$ denotes the covariance matrix associated with the radar signal $\mathbf{x}_0$, which must satisfy the positive semi-definite property [48].

III. Joint Beamforming and Power Splitting Optimization with Perfect CSI

To remove the min function in (9), we first introduce an auxiliary variable $e = \min_{k\in\mathcal{K}} E_k$ to recast it as the following equivalent problem

$$\underset{\{\mathbf{w}_k,\alpha_k,\mathbf{S}_0,\Gamma,e\}}{\text{maximize}} \quad e \tag{10a}$$

$$\text{s.t.} \quad E_k \ge e, \forall k \in \mathcal{K}, \tag{10b}$$

$$\text{C1-C6.} \tag{10c}$$

Since the optimization variables $\{\mathbf{w}_k, \alpha_k, \mathbf{S}_0, \Gamma\}$ are highly coupled in the problem (10), the block coordinate descent method is exploited to alternately optimize the transmit beamformer at the BS, phase shifts of IRS, and power splitting ratios of users, as detailed in the following subsections [55]. In summary, the flowchart for solving the harvested power maximization problem (9) is shown in Fig. 2.

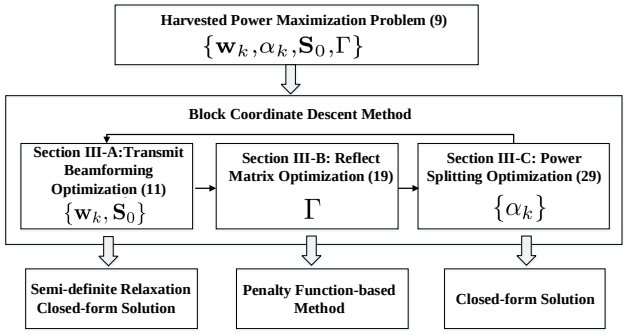

Fig. 2: The flowchart for solving (9).

A. Transmit Beamforming Optimization Subproblem

Given $\{\Gamma^*, \alpha_k^*\}$, we can rewrite (10) as the following transmit beamforming optimization subproblem

$$\underset{\{\mathbf{w}_k,\mathbf{S}_0,e\}}{\text{maximize}} \quad e \tag{11a}$$

$$\text{s.t.} \quad \frac{|\mathbf{h}_k^H\mathbf{w}_k|^2}{\sum_{i=1,i\neq k}^{K} |\mathbf{h}_k^H\mathbf{w}_i|^2 + \mathbf{h}_k^H\mathbf{S}_0\mathbf{h}_k + \delta_k^2 + \frac{\zeta_k^2}{\alpha_k^*}} \ge \gamma_{\min,k}, \forall k \in \mathcal{K}, \tag{11b}$$

$$\eta_k(1-\alpha_k^*)(\mathbf{h}_k^H\mathbf{S}_0\mathbf{h}_k+\sum_{i=1}^{K}|\mathbf{h}_k^H\mathbf{w}_i|^2+\delta_k^2) \geq e, \forall k\in\mathcal{K}, \tag{11c}$$

$$\mathbf{a}^H(\phi_l)\left(\mathbf{S}_0+\sum_{k=1}^{K}\mathbf{w}_k\mathbf{w}_k^H\right)\mathbf{a}(\phi_l)\geq b_{\min,l}, \forall l\in\mathcal{L}, \tag{11d}$$

$$\text{C1, C6.} \tag{11e}$$

Defining $\mathbf{W}_k = \mathbf{w}_k\mathbf{w}_k^H$, we have $|\mathbf{h}_k^H\mathbf{w}_i|^2 = \mathbf{w}_i^H\mathbf{h}_k\mathbf{h}_k^H\mathbf{w}_i = \text{Tr}(\mathbf{h}_k\mathbf{h}_k^H\mathbf{w}_i\mathbf{w}_i^H) = \text{Tr}(\mathbf{H}_k\mathbf{W}_i)$, $\mathbf{h}_k^H\mathbf{S}_0\mathbf{h}_k = \text{Tr}(\mathbf{H}_k\mathbf{S}_0)$, and $\mathbf{a}^H(\phi_l)\left(\mathbf{S}_0+\sum_{k=1}^{K}\mathbf{w}_k\mathbf{w}_k^H\right)\mathbf{a}(\phi_l) = \text{Tr}\left(\mathbf{A}(\phi_l)\left(\mathbf{S}_0+\sum_{k=1}^{K}\mathbf{W}_k\right)\right)$, where $\mathbf{H}_k = \mathbf{h}_k\mathbf{h}_k^H$ and $\mathbf{A}(\phi_l) = \mathbf{a}(\phi_l)\mathbf{a}(\phi_l)^H$. Hence, (11) can be converted to the following problem

$$\underset{\{\mathbf{W}_k,\mathbf{S}_0,e\}}{\text{maximize}} \quad e \tag{12a}$$

$$\text{s.t.} \quad \frac{\text{Tr}(\mathbf{H}_k\mathbf{W}_k)}{\gamma_{\min,k}} \geq \sum_{i=1,i\neq k}^{K}\text{Tr}(\mathbf{H}_k\mathbf{W}_i)+\text{Tr}(\mathbf{H}_k\mathbf{S}_0)+\delta_k^2+\frac{\zeta_k^2}{\alpha_k^*}, \forall k\in\mathcal{K}, \tag{12b}$$

$$\text{Tr}(\mathbf{H}_k\mathbf{S}_0)+\sum_{i=1}^{K}\text{Tr}(\mathbf{H}_k\mathbf{W}_i)+\delta_k^2 \geq \frac{e}{\eta_k(1-\alpha_k^*)}, \forall k\in\mathcal{K}, \tag{12c}$$

$$\text{Tr}\left(\mathbf{A}(\phi_l)\left(\mathbf{S}_0+\sum_{k=1}^{K}\mathbf{W}_k\right)\right)\geq b_{\min,l}, \forall l\in\mathcal{L}, \tag{12d}$$

$$\text{Rank}(\mathbf{W}_k)=1, \forall k\in\mathcal{K}, \tag{12e}$$

$$\mathbf{S}_0\succeq 0, \mathbf{W}_k\succeq 0, \forall k\in\mathcal{K}, \tag{12f}$$

$$\text{Tr}(\mathbf{S}_0)+\sum_{k=1}^{K}\text{Tr}(\mathbf{W}_k)\leq P_{\max,B}. \tag{12g}$$

Problem (12) is still non-convex because of the rank-one constraint (12e). By employing the semi-definite relaxation technique [56], this article eliminates the rank-one constraint to transform (12) to a convex problem. Consequently, it becomes amenable to solution using conventional convex optimization methods incorporated within CVX [57]. Besides, the subsequent theorem establishes the tightness of the rank-one relaxation and demonstrates that the optimal transmit beamforming strategy can be restored by leveraging equations (13)-(14).

Proposition 1: Suppose that the optimal solution $\{\mathbf{W}_k^*, \mathbf{S}_0^*, e^*\}$ satisfies $\text{Rank}(\mathbf{W}_k^*)>1$, we can construct the feasible solution $\{\hat{\mathbf{W}}_k, \hat{\mathbf{S}}_0, e^*\}$ of (12) to achieve the optimal harvested power of users, in which

$$\hat{\mathbf{W}}_k = \hat{\mathbf{w}}_k\hat{\mathbf{w}}_k^H, \tag{13}$$

$$\hat{\mathbf{S}}_0 = \sum_{k=1}^{K}\mathbf{W}_k^*+\mathbf{S}_0^*-\sum_{k=1}^{K}\hat{\mathbf{W}}_k, \tag{14}$$

where $\hat{\mathbf{w}}_k = \frac{1}{\sqrt{\mathbf{h}_k^H\mathbf{W}_k^*\mathbf{h}_k}}\mathbf{W}_k^*\mathbf{h}_k$.

Proof: Since $\sum_{k=1}^{K}\hat{\mathbf{W}}_k+\hat{\mathbf{S}}_0 = \sum_{k=1}^{K}\mathbf{W}_k^*+\mathbf{S}_0^*$, we can derive that the solution of $\{\hat{\mathbf{W}}_k, \hat{\mathbf{S}}_0, e_k^*\}$, satisfies the constraints (12c), (12d) and (12g), and it can achieve the identical objective function e^* compared to the counterpart achieved by the solution of $\{\mathbf{W}_k^*, \mathbf{S}_0^*, e^*\}$.

Furthermore, we will prove that the solution $\{\hat{\mathbf{W}}_k, \hat{\mathbf{S}}_0, e_k^*\}$ satisfies (12f). As observed, $\hat{\mathbf{W}}_k$ is positive semi-definite and rank-one matrix. For an arbitrary $\mathbf{g}\in\mathbb{C}^{M\times 1}$, we have

$$\begin{aligned}&\mathbf{g}^H(\mathbf{W}_k^*-\hat{\mathbf{W}}_k)\mathbf{g} = \mathbf{g}^H\mathbf{W}_k^*\mathbf{g}-\\ &\mathbf{g}^H\frac{1}{\sqrt{\mathbf{h}_k^H\mathbf{W}_k^*\mathbf{h}_k}}\mathbf{W}_k^*\mathbf{h}_k(\frac{1}{\sqrt{\mathbf{h}_k^H\mathbf{W}_k^*\mathbf{h}_k}}\mathbf{W}_k^*\mathbf{h}_k)^H\mathbf{g}\\ &=\mathbf{g}^H\mathbf{W}_k^*\mathbf{g}-\frac{|\mathbf{h}_k^H\mathbf{W}_k^*\mathbf{g}|^2}{\mathbf{h}_k^H\mathbf{W}_k^*\mathbf{h}_k}\\ &\overset{(a)}{\geq}\mathbf{g}^H\mathbf{W}_k^*\mathbf{g}-\frac{(\mathbf{h}_k^H\mathbf{W}_k^*\mathbf{h}_k)(\mathbf{g}^H\mathbf{W}_k^*\mathbf{g})}{\mathbf{h}_k^H\mathbf{W}_k^*\mathbf{h}_k}=0,\end{aligned} \tag{15}$$

where (a) holds according to the Cauchy-Schwarz inequality, i.e., $|\mathbf{h}_k^H\mathbf{W}_k^*\mathbf{g}|^2\leq(\mathbf{h}_k^H\mathbf{W}_k^*\mathbf{h}_k)(\mathbf{g}^H\mathbf{W}_k^*\mathbf{g})$. Therefore, it follows that $\mathbf{W}_k^*-\hat{\mathbf{W}}_k\succeq 0$ and $\sum_{k=1}^{K}(\mathbf{W}_k^*-\hat{\mathbf{W}}_k)\succeq 0$. Meanwhile, since $\mathbf{S}_0^*\succeq 0$, we can derive that $\hat{\mathbf{S}}_0 = \sum_{k=1}^{K}(\mathbf{W}_k^*-\hat{\mathbf{W}}_k)+\mathbf{S}_0^*\succeq 0$.

Finally, we will prove that the solution satisfies (12b). According to (13)-(14), we have

$$\begin{aligned}&\text{Tr}(\mathbf{H}_k\hat{\mathbf{W}}_k) = \mathbf{h}_k^H\hat{\mathbf{w}}_k\hat{\mathbf{w}}_k^H\mathbf{h}_k\\ &=\mathbf{h}_k^H\frac{1}{\sqrt{\mathbf{h}_k^H\mathbf{W}_k^*\mathbf{h}_k}}\mathbf{W}_k^*\mathbf{h}_k(\frac{1}{\sqrt{\mathbf{h}_k^H\mathbf{W}_k^*\mathbf{h}_k}}\mathbf{W}_k^*\mathbf{h}_k)^H\mathbf{h}_k\\ &=\mathbf{h}_k^H\mathbf{W}_k^*\mathbf{h}_k=\text{Tr}(\mathbf{H}_k\mathbf{W}_k^*),\end{aligned} \tag{16}$$

and

$$\hat{\mathbf{S}}_0+\sum_{k=1}^{K}\hat{\mathbf{W}}_k = \sum_{k=1}^{K}\mathbf{W}_k^*+\mathbf{S}_0^*. \tag{17}$$

Hence, we have

$$\begin{aligned}&\frac{1+\gamma_{\min,k}}{\gamma_{\min,k}}\text{Tr}(\mathbf{H}_k\hat{\mathbf{W}}_k)\overset{(\beta_1)}{=}\frac{1+\gamma_{\min,k}}{\gamma_{\min,k}}\text{Tr}(\mathbf{H}_k\mathbf{W}_k^*)\\ &\overset{(\beta_2)}{\geq}\sum_{i=1}^{K}\text{Tr}(\mathbf{H}_k\mathbf{W}_i^*)+\text{Tr}(\mathbf{H}_k\mathbf{S}_0^*)+\delta_k^2+\frac{\zeta_k^2}{\alpha_k^*}\\ &\overset{(\beta_3)}{=}\sum_{i=1}^{K}\text{Tr}(\mathbf{H}_k\hat{\mathbf{W}}_i)+\text{Tr}(\mathbf{H}_k\hat{\mathbf{S}}_0)+\delta_k^2+\frac{\zeta_k^2}{\alpha_k^*},\end{aligned} \tag{18}$$

where (β_1) and (β_3) hold according to (16) and (17), respectively, and (β_2) establishes since the optimal solution $\{\mathbf{W}_k^*, \mathbf{S}_0^*, e^*\}$ of (12) should satisfy (12b). By subtracting $\text{Tr}(\mathbf{H}_k\hat{\mathbf{W}}_k)$ on both the left and right sides of (18), we derive that the solution $\{\hat{\mathbf{W}}_k, \hat{\mathbf{S}}_0, e^*\}$ also satisfies (12b). Based on above descriptions, we complete the proof.

Remark 2: Proposition 1 demonstrates that we can always find a solution $\{\hat{\mathbf{W}}_k, \hat{\mathbf{S}}_0\}$ via (13)-(14) to achieve the same minimum harvested power among all users, as compared to the optimal solution of (12) without rank-one constraint (12e). Therefore, the rank-one relaxation is tight[7].

B. Reflect Matrix Optimization Subproblem

Given $\{\mathbf{w}_k^*, \alpha_k^*, \mathbf{S}_0^*\}$, (10) can be streamlined into the reflect matrix optimization subproblem

$$\underset{\{\Gamma, e\}}{\text{maximize}} \quad e \tag{19a}$$

$$\text{s.t.} \quad \frac{|\mathbf{h}_k^H \mathbf{w}_k^*|^2}{\sum_{i=1, i\neq k}^{K} |\mathbf{h}_k^H \mathbf{w}_i^*|^2 + \mathbf{h}_k^H \mathbf{S}_0^* \mathbf{h}_k + \delta_k^2 + \frac{\zeta_k^2}{\alpha_k^*}} \geq \gamma_{\min,k}, \forall k \in \mathcal{K}, \tag{19b}$$

$$\eta_k(1-\alpha_k^*)(\mathbf{h}_k^H \mathbf{S}_0^* \mathbf{h}_k + \sum_{i=1}^{K} |\mathbf{h}_k^H \mathbf{w}_i^*|^2 + \delta_k^2) \geq e, \forall k \in \mathcal{K}, \tag{19c}$$

$$0 \leq \theta_n \leq 2\pi, \forall n \in \mathcal{N}, \tag{19d}$$

where $\mathbf{h}_k^H = \mathbf{h}_{d,k}^H + \mathbf{h}_{r,k}^H \Gamma \mathbf{G}$. Defining $\mathbf{v} = [e^{j\theta_1}, e^{j\theta_2}, \cdots, e^{j\theta_N}]$, $\hat{\mathbf{v}} = [\mathbf{v}, 1]$ and $\hat{\mathbf{V}} = \hat{\mathbf{v}}^H \hat{\mathbf{v}}$, we have

$$\begin{aligned}
&|\mathbf{h}_k^H \mathbf{w}_i^*|^2 = |(\mathbf{h}_{d,k}^H + \mathbf{h}_{r,k}^H \Gamma \mathbf{G}) \mathbf{w}_i^*|^2 = |(\mathbf{h}_{d,k}^H + \mathbf{v}\text{diag}\{\mathbf{h}_{r,k}^H\}\mathbf{G})\mathbf{w}_i^*|^2 \\
&= \left| [\mathbf{v}, 1] \begin{bmatrix} \text{diag}\{\mathbf{h}_{r,k}^H\}\mathbf{G}\mathbf{w}_i^* \\ \mathbf{h}_{d,k}^H \mathbf{w}_i^* \end{bmatrix} \right|^2 = \left| \hat{\mathbf{v}} \begin{bmatrix} \text{diag}\{\mathbf{h}_{r,k}^H\}\mathbf{G}\mathbf{w}_i^* \\ \mathbf{h}_{d,k}^H \mathbf{w}_i^* \end{bmatrix} \right|^2 = \\
&\hat{\mathbf{v}} \begin{bmatrix} \text{diag}\{\mathbf{h}_{r,k}^H\}\mathbf{G}\mathbf{w}_i^* \\ \mathbf{h}_{d,k}^H \mathbf{w}_i^* \end{bmatrix} \left[(\mathbf{w}_i^*)^H \mathbf{G}^H \text{diag}\{\mathbf{h}_{r,k}\}, (\mathbf{w}_i^*)^H \mathbf{h}_{d,k} \right] \hat{\mathbf{v}}^H \\
&= \hat{\mathbf{v}} \mathbf{R}_{k,i} \hat{\mathbf{v}}^H = \text{Tr}(\mathbf{R}_{k,i} \hat{\mathbf{V}}),
\end{aligned} \tag{20}$$

where

$$\mathbf{R}_{k,i} = \begin{bmatrix} \text{diag}\{\mathbf{h}_{r,k}^H\}\mathbf{G}\mathbf{W}_i^*\mathbf{G}^H\text{diag}\{\mathbf{h}_{r,k}\} & \text{diag}\{\mathbf{h}_{r,k}^H\}\mathbf{G}\mathbf{W}_i^*\mathbf{h}_{d,k} \\ \mathbf{h}_{d,k}^H\mathbf{W}_i^*\mathbf{G}^H\text{diag}\{\mathbf{h}_{r,k}\} & \mathbf{h}_{d,k}^H\mathbf{W}_i^*\mathbf{h}_{d,k} \end{bmatrix}. \tag{21}$$

Similarly, we can derive that

$$\mathbf{h}_k^H \mathbf{S}_0^* \mathbf{h}_k = \text{Tr}(\mathbf{Z}_k \hat{\mathbf{V}}), \tag{22}$$

where

$$\mathbf{Z}_k = \begin{bmatrix} \text{diag}\{\mathbf{h}_{r,k}^H\}\mathbf{G}\mathbf{S}_0^*\mathbf{G}^H\text{diag}\{\mathbf{h}_{r,k}\} & \text{diag}\{\mathbf{h}_{r,k}^H\}\mathbf{G}\mathbf{S}_0^*\mathbf{h}_{d,k} \\ \mathbf{h}_{d,k}^H\mathbf{S}_0^*\mathbf{G}^H\text{diag}\{\mathbf{h}_{r,k}\} & \mathbf{h}_{d,k}^H\mathbf{S}_0^*\mathbf{h}_{d,k} \end{bmatrix}. \tag{23}$$

[7]Unlike the literature in [21] and [58] that considers IRS-aided SWIPT systems, the information and energy bemaforming strategies proposed in these works cannot be directly applied to solve problem (11), due to the existence of sensing beamforming $\mathbf{S}_0$ and minimum sensing beampattern constraints (11d). In addition to proving that rank-one relaxation is tight, we provide the closed-form solution structure of the optimal transmit beamforming $\{\mathbf{w}_k^*, \mathbf{S}_0^*\}$.

According to (20)-(23), we can rewrite the phase shift optimization subproblem as

$$\underset{\{\hat{\mathbf{V}} \succeq 0, e\}}{\text{maximize}} \quad e \tag{24a}$$

$$\begin{aligned}
\text{s.t.} \quad & \frac{\text{Tr}(\mathbf{R}_{k,k}\hat{\mathbf{V}})}{\gamma_{\min,k}} \geq \sum_{i=1, i\neq k}^{K} \text{Tr}(\mathbf{R}_{k,i}\hat{\mathbf{V}}) + \\
& \text{Tr}(\mathbf{Z}_k\hat{\mathbf{V}}) + \delta_k^2 + \frac{\zeta_k^2}{\alpha_k^*}, \forall k \in \mathcal{K},
\end{aligned} \tag{24b}$$

$$\text{Tr}(\mathbf{Z}_k\hat{\mathbf{V}}) + \sum_{i=1}^{K} \text{Tr}(\mathbf{R}_{k,i}\hat{\mathbf{V}}) + \delta_k^2 \geq \frac{e}{\eta_k(1-\alpha_k^*)}, \forall k \in \mathcal{K}, \tag{24c}$$

$$\hat{\mathbf{V}}_{n,n} = 1, \forall n \in \{\mathcal{N}, N+1\}, \tag{24d}$$

$$\text{Rank}(\hat{\mathbf{V}}) = 1. \tag{24e}$$

Next, we will tackle the non-concave and non-convex rank-one constraint (24e). An equivalent form for (24e) will be $\text{Tr}(\hat{\mathbf{V}}) = \lambda_{\max}(\hat{\mathbf{V}})$, where $\lambda_{\max}(\hat{\mathbf{V}})$ denotes the maximum eigenvalue of $\hat{\mathbf{V}}$. As expected, the inequality $\text{Tr}(\hat{\mathbf{V}}) \geq \lambda_{\max}(\hat{\mathbf{V}})$ holds for any $\hat{\mathbf{V}} \succeq 0$, and the equality holds when the rank of $\hat{\mathbf{V}}$ is equal to 1. Hence, (24) is converted as

$$\underset{\{\hat{\mathbf{V}} \succeq 0, e\}}{\text{maximize}} \quad e - \nu(\text{Tr}(\hat{\mathbf{V}}) - \lambda_{\max}(\hat{\mathbf{V}})) \tag{25a}$$

$$\text{s.t.} \quad \text{(24b)-(24d)}, \tag{25b}$$

where $\nu \geq 0$ is the penalty factor. The following lemma demonstrates the equivalence of problems (24) and (25).

Lemma 1: Let $\hat{\mathbf{V}}^{(i)}$ denote the optimal solution of problem (25) at the i-th iteration. When penalty factor ν is sufficiently large, i.e., $\nu \to +\infty$, then any limit point of sequence $\{\hat{\mathbf{V}}^{(i)}\}$ is an optimal solution of problem (24).

Proof: The similar proof can be found in *Proposition 2* of [59].

Next, we will tackle the non-convex and non-concave objective function (25a). According to *Lemma 2* in [60], we derive the lower bound of $\lambda_{\max}(\hat{\mathbf{V}})$ as

$$\lambda_{\max}(\hat{\mathbf{V}}) \geq \lambda_{\max}(\hat{\mathbf{V}}^{(i-1)}) + (\hat{\mathbf{v}}_{\max}^{(i-1)})^H (\hat{\mathbf{V}} - \hat{\mathbf{V}}^{(i-1)}) \hat{\mathbf{v}}_{\max}^{(i-1)}, \tag{26}$$

where $\hat{\mathbf{V}}^{(i-1)}$ represents the optimal $\hat{\mathbf{V}}$ at the $(i-1)$-th iteration, $\hat{\mathbf{v}}_{\max}^{(i-1)}$ denotes the unit eigenvector related to maximum eigenvalue $\lambda_{\max}(\hat{\mathbf{V}}^{(i-1)})$ of $\hat{\mathbf{V}}^{(i-1)}$. Replacing $\lambda_{\max}(\hat{\mathbf{V}})$ as its lower bound and removing the constant term $\lambda_{\max}(\hat{\mathbf{V}}^{(i-1)}) - (\hat{\mathbf{v}}_{\max}^{(i-1)})^H \hat{\mathbf{V}}^{(i-1)} \hat{\mathbf{v}}_{\max}^{(i-1)}$, (25) can be tackled by iteratively solving the following problem

$$\underset{\{\hat{\mathbf{V}} \succeq 0, e\}}{\text{maximize}} \quad e - \nu(\text{Tr}(\hat{\mathbf{V}}) - (\hat{\mathbf{v}}_{\max}^{(i-1)})^H \hat{\mathbf{V}} \hat{\mathbf{v}}_{\max}^{(i-1)}) \tag{27a}$$

$$\text{s.t.} \quad \text{(24b)-(24d)}. \tag{27b}$$

As observed, the classic convex toolbox, such as CVX, can be called to solve the convex optimization problem (27). The proposed penalty function-based method for solving the IRS phase shift optimization subproblem is summarized in Algorithm 1.

Lemma 2: Algorithm 1 generates a sequence $\{\hat{\mathbf{V}}^{(i)}\}$ with

Algorithm 1: Penalty function-based method to solve reflect matrix optimization subproblem (19)

% **Initialization stage**:
Choose a proper penalty factor ν, and a feasible solution $\hat{\mathbf{V}}^{(0)}$. Set iteration factor $i=1$, and tolerance factor ι.
Repeat:
  Obtain the optimal $\hat{\mathbf{V}}^{(i)}$ by solving (27);
  If $\hat{\mathbf{V}}^{(i)}=\hat{\mathbf{V}}^{(i-1)}$ (i.e., no improved solution found) then
    set $\nu=2\nu$;
  end if
  Update iteration factor $i=i+1$;
Until $\frac{\mathrm{Tr}(\hat{\mathbf{V}}^{(i)})-\lambda_{\max}(\hat{\mathbf{V}}^{(i)})}{\mathrm{Tr}(\hat{\mathbf{V}}^{(i)})}\leq\iota$.
% **Optimization stage**:
Set $i=1$;
Repeat:
  Obtain the optimal $\hat{\mathbf{V}}^{(i)}$ by solving (27);
  Update iteration factor $i=i+1$;
Until $\frac{\mathrm{Tr}(\hat{\mathbf{V}}^{(i)})-\lambda_{\max}(\hat{\mathbf{V}}^{(i)})}{\mathrm{Tr}(\hat{\mathbf{V}}^{(i)})}\leq\iota$.
Output: optimal solution Γ^*.

improved solution of problem (25), which converges to a solution satisfying first-order necessary optimality condition.

Proof: Suppose that $\hat{\mathbf{V}}^{(i)}$ is the optimal solution of (26) at the i-th iteration. Given $\{\mathbf{w}_k^{(n)},\mathbf{S}_0^{(n)},\alpha_k^{(n)}\}$, let us denote $e(\hat{\mathbf{V}}^{(i)})=\max\limits_{k\in\mathcal{K}} E_k(\mathbf{w}_k^{(n)},\mathbf{S}_0^{(n)},\hat{\mathbf{V}}^{(i)},\alpha_k^{(n)})$. Therefore, we have

$$\begin{aligned}&e(\hat{\mathbf{V}}^{(i+1)})-\nu(\mathrm{Tr}(\hat{\mathbf{V}}^{(i+1)})-\lambda_{\max}(\hat{\mathbf{V}}^{(i+1)}))\overset{(a1)}{\geq} e(\hat{\mathbf{V}}^{(i+1)})-\\ &\nu(\mathrm{Tr}(\hat{\mathbf{V}}^{(i+1)})-\lambda_{\max}(\hat{\mathbf{V}}^{(i)})-(\hat{\mathbf{v}}_{\max}^{(i)})^H(\hat{\mathbf{V}}^{(i+1)}-\hat{\mathbf{V}}^{(i)})\hat{\mathbf{v}}_{\max}^{(i)})\overset{(a2)}{\geq}\\ &e(\hat{\mathbf{V}}^{(i)})-\nu(\mathrm{Tr}(\hat{\mathbf{V}}^{(i)})-\lambda_{\max}(\hat{\mathbf{V}}^{(i)})-(\hat{\mathbf{v}}_{\max}^{(i)})^H(\hat{\mathbf{V}}^{(i)}-\hat{\mathbf{V}}^{(i)})\hat{\mathbf{v}}_{\max}^{(i)})\\ &=e(\hat{\mathbf{V}}^{(i)})-\nu(\mathrm{Tr}(\hat{\mathbf{V}}^{(i)})-\lambda_{\max}(\hat{\mathbf{V}}^{(i)})),\end{aligned}\tag{28}$$

where $(a1)$ holds according to Eq. (26), i.e., $\lambda_{\max}(\hat{\mathbf{V}}^{(i+1)})\geq\lambda_{\max}(\hat{\mathbf{V}}^{(i)})+(\hat{\mathbf{v}}_{\max}^{(i)})^H(\hat{\mathbf{V}}^{(i+1)}-\hat{\mathbf{V}}^{(i)})\hat{\mathbf{v}}_{\max}^{(i)}$, $(a2)$ holds because that the optimal $\{\hat{\mathbf{V}}^{(i+1)}\}$ is generated by maximizing (27a). Hence, the optimal objective function (27a) demonstrates non-decreasing behavior with each iteration. Integrated with the assurance of the boundedness of the optimal value of (27), Algorithm 1 is ensured to converge to a solution that satisfies first-order necessary optimality condition, according to Proposition 1 in [61].

C. Power Splitting Optimization Subproblem

Given $\{\mathbf{w}_k^*,\mathbf{S}_0^*,\Gamma^*\}$, (10) can be reduced to the following power splitting optimization subproblem

$$\begin{aligned}\underset{\{\alpha_k\}}{\text{maximize}}\quad &\min_{k\in\mathcal{K}}\ \eta_k(1-\alpha_k)(\mathrm{Tr}(\mathbf{H}_k\mathbf{S}_0^*)+\sum_{i=1}^{K}\mathrm{Tr}(\mathbf{H}_k\mathbf{W}_i^*)\\ &+\delta_k^2)\end{aligned}\tag{29a}$$

$$\text{s.t.}\quad \frac{\alpha_k\mathrm{Tr}(\mathbf{H}_k\mathbf{W}_k^*)}{\gamma_{\min,k}}\geq\sum_{i=1,i\neq k}^{K}\alpha_k\mathrm{Tr}(\mathbf{H}_k\mathbf{W}_i^*)+\tag{29b}$$

$$\alpha_k\mathrm{Tr}(\mathbf{H}_k\mathbf{S}_0^*)+\alpha_k\delta_k^2+\zeta_k^2,\forall k\in\mathcal{K},$$

$$0\leq\alpha_k\leq 1,\forall k\in\mathcal{K}.\tag{29c}$$

To reduce the computational complexity, we deduce closed-form expressions for the optimal power splitting ratios, as presented in the following *Proposition 2*.

Proposition 2: For power splitting optimization subproblem (29), the minimum harvested power among all users will be maximized when users adopt the following power splitting ratios:

$$\alpha_k^*=\left[\frac{\zeta_k^2}{\frac{\mathrm{Tr}(\mathbf{H}_k\mathbf{W}_k^*)}{\gamma_{\min,k}}-\sum\limits_{i=1,i\neq k}^{K}\mathrm{Tr}(\mathbf{H}_k\mathbf{W}_i^*)-\mathrm{Tr}(\mathbf{H}_k\mathbf{S}_0^*)-\delta_k^2}\right]^+,$$
$$\forall k\in\mathcal{K},\tag{30}$$

where $[x]^+=\max\{x,0\}$.

Proof: After some inequality transformations, (29b) is rewritten as

$$\alpha_k\geq\frac{\zeta_k^2}{\frac{\mathrm{Tr}(\mathbf{H}_k\mathbf{W}_k^*)}{\gamma_{\min,k}}-\sum\limits_{i=1,i\neq k}^{K}\mathrm{Tr}(\mathbf{H}_k\mathbf{W}_i^*)-\mathrm{Tr}(\mathbf{H}_k\mathbf{S}_0^*)-\delta_k^2}.\tag{31}$$

Integrated with (29c), we can transform the (29) to the following problem

$$\begin{aligned}\underset{\{\alpha_k\}}{\text{maximize}}\quad &\min_{k\in\mathcal{K}}\ \eta_k(1-\alpha_k)(\mathrm{Tr}(\mathbf{H}_k\mathbf{S}_0^*)+\sum_{i=1}^{K}\mathrm{Tr}(\mathbf{H}_k\mathbf{W}_i^*)+\delta_k^2)\end{aligned}\tag{32a}$$

$$\begin{aligned}\text{s.t.}\quad &\left[\frac{\zeta_k^2}{\frac{\mathrm{Tr}(\mathbf{H}_k\mathbf{W}_k^*)}{\gamma_{\min,k}}-\sum\limits_{i=1,i\neq k}^{K}\mathrm{Tr}(\mathbf{H}_k\mathbf{W}_i^*)-\mathrm{Tr}(\mathbf{H}_k\mathbf{S}_0^*)-\delta_k^2}\right]^+\\ &\leq\alpha_k\leq 1,\forall k\in\mathcal{K}.\end{aligned}\tag{32b}$$

As seen in (32a), the power harvested by the k-th user increases as the power splitting ratio α_k decreases. Consequently, when each user adopts its lower bound of power splitting ratio, the optimal objective function of (29) will be obtained.

Based on the analysis above, we outline the proposed method for solving the formulated non-convex problem (9)

in Algorithm 1 below. As expected, the initialization of IRS phase shift matrix $\Gamma^{(0)}$ and power splitting ratios $\{\alpha_k^{(0)}\}$ is crucial to ensure the feasibility of the transmit beamforming optimization subproblem (12) at step 3. According to proposition 3.1 in [10], the SINR constraints of (12) will be satisfied when $\sum_{k=1}^{K} \frac{\gamma_{\min,k}}{1+\gamma_{\min,k}} \leq \text{Rank}(\mathbf{H})$, where $\mathbf{H} = [\mathbf{h}_1, \mathbf{h}_2, \cdots, \mathbf{h}_K]^H = \mathbf{h}_{r,k}^H \Gamma^{(0)} \mathbf{G} + \mathbf{h}_{d,k}^H, \forall k \in \mathcal{K}$. Meanwhile, the BS transmit power restrictions and minimum sensing beampattern gain requirements are independent of $\Gamma^{(0)}$ and $\{\alpha_k^{(0)}\}$, and can be met by adjusting the transmit beamforming strategy. Therefore, before the block coordinate descent (BCD) iteration, we need to initialize IRS phase shift matrix $\Gamma^{(0)}$ and power splitting ratios $\{\alpha_k^{(0)}\}$, and verify whether the feasibility condition $\sum_{k=1}^{K} \frac{\gamma_{\min,k}}{1+\gamma_{\min,k}} \leq \text{Rank}(\mathbf{H})$ is satisfied.

Algorithm 2: Alternating optimization method to solve (9)

1 Set the iteration factor $n = 1$. Initialize $\{\Gamma^{(0)}, \alpha_k^{(0)}\}$.
2 **Repeat:**
3 Calculate $\{\mathbf{w}_k^{(n)}, \mathbf{S}_0^{(n)}\}$ by solving (12);
4 Acquire $\Gamma^{(n)}$ by solving (19) with penalty function-based method;
5 Compute $\{\alpha_k^{(n)}\}$ according to *Proposition 2*;
6 Update iteration factor $n = n + 1$;
7 **Until** convergence.
8 **Output:** optimal solution $(\mathbf{w}_k^*, \mathbf{S}_0^*, \Gamma^*, \alpha_k^*)$.

Next, we will analyze the convergence of Algorithm 2. Assuming $\Gamma^{(n)}$, $\{\alpha_k^{(n)}\}$ and $\{\mathbf{w}_k^{(n)}, \mathbf{S}_0^{(n)}\}$ as the optimal IRS reflection matrix, power splitting ratios and transmit beamforming of BS at the n-th iteration, respectively. In step 3 of Algorithm 2, the optimal transmit beamforming strategy is obtained by solving (12), we have

$$e(\mathbf{w}_k^{(n)}, \mathbf{S}_0^{(n)}, \Gamma^{(n)}, \alpha_k^{(n)}) \leq e(\mathbf{w}_k^{(n+1)}, \mathbf{S}_0^{(n+1)}, \Gamma^{(n)}, \alpha_k^{(n)}), \tag{33}$$

where e denotes the minimum harvested power of users, and it is defined in the first paragraph of Section III. Given $\{\mathbf{w}_k^{(n+1)}, \mathbf{S}_0^{(n+1)}, \alpha_k^{(n)}\}$, in step 4 of Algorithm 2, we have

$$\begin{aligned} &e(\mathbf{w}_k^{(n+1)}, \mathbf{S}_0^{(n+1)}, \Gamma^{(n)}, \alpha_k^{(n)}) \\ &\leq e(\mathbf{w}_k^{(n+1)}, \mathbf{S}_0^{(n+1)}, \Gamma^{(n+1)}, \alpha_k^{(n)}). \end{aligned} \tag{34}$$

Finally, given $\{\mathbf{w}_k^{(n+1)}, \mathbf{S}_0^{(n+1)}, \Gamma^{(n+1)}\}$, the optimal power splitting ratios are acquired via *Proposition 3*, it yields that

$$\begin{aligned} &e(\mathbf{w}_k^{(n+1)}, \mathbf{S}_0^{(n+1)}, \Gamma^{(n+1)}, \alpha_k^{(n)}) \\ &\leq e(\mathbf{w}_k^{(n+1)}, \mathbf{S}_0^{(n+1)}, \Gamma^{(n+1)}, \alpha_k^{(n+1)}). \end{aligned} \tag{35}$$

According to (32)-(34), we obtain

$$e(\mathbf{w}_k^{(n)}, \mathbf{S}_0^{(n)}, \Gamma^{(n)}, \alpha_k^{(n)}) \leq e(\mathbf{w}_k^{(n+1)}, \mathbf{S}_0^{(n+1)}, \Gamma^{(n+1)}, \alpha_k^{(n+1)}), \tag{36}$$

which implies that the solution to problem (9) is non-decreasing after each iteration of the BCD method. Since the harvested power of users is inherently bounded by the circuit architecture and the maximum transmit power of the BS, it is constrained to a finite value. Consequently, the convergence of Algorithm 2 is assured.

Then, the computational complexity of Algorithm 2 is analyzed as follows. Defining I_1 and I_2 as the iteration number of Algorithms 1-2, respectively. In step 3, the optimal transmit beamformer is acquired by solving problem (12), which involves $3K+L+2$ constraints and $(K+1)M^2+1$ variables. The computational complexity of this step is written as $\mathcal{O}(((K+1)M^2+3K+L+3)((K+1)M^2+1)^2\sqrt{3K+L+2}\log(\frac{1}{\epsilon_1}))$, where ϵ_1 represents the tolerance coefficient. In step 4, the optimal IRS phase shifts will be obtained by iteratively solving convex problem (27), and the computational complexity of this step is given by $\mathcal{O}(I_1((N+1)^2+2K+2)((N+1)^2+1)^2\sqrt{2K+1}\log(\frac{1}{\epsilon_2}))$, where ϵ_2 indicates the corresponding tolerance coefficient. In step 5, the optimal power splitting ratio is calculated using (30), with complexity $\mathcal{O}(K)$. Combining all steps, the total computational complexity of Algorithm 2 is given by $\mathcal{O}(I_2(((K+1)M^2+3K+L+3)((K+1)M^2+1)^2\sqrt{3K+L+2}\log(\frac{1}{\epsilon_1})+I_1((N+1)^2+2K+2)((N+1)^2+1)^2\sqrt{2K+1}\log(\frac{1}{\epsilon_2})+K))$.

D. Minimum Harvested Power Maximization Problem with Non-linear Power Harvesting Model

The preceding subsections analyzed the beamforming optimization under the assumption of a linear power harvesting model. To accommodate non-linear power harvesting characteristics, we now consider the following non-linear power harvesting model:

$$E_k^{\text{NL}} = \frac{\Psi_k - P_{\text{sat}}\Delta}{1-\Delta}, \forall k \in \mathcal{K}, \tag{37}$$

where E_k^{NL} represents the power harvested by k-th user, $\Delta = \frac{1}{1+\exp(ab)}$, $\Psi_k = \frac{P_{\text{sat}}}{1+\exp(-a(P_{\text{EH},k}-b))}$, and $P_{\text{EH},k} = (1-\alpha_k)(\mathbf{h}_k^H \mathbf{S}_0 \mathbf{h}_k + \sum_{i=1}^{K} |\mathbf{h}_k^H \mathbf{w}_i|^2 + \delta_k^2)$. Noted that P_{sat} represents the maximum harvested power at k-th user, a and b are parameters related to circuit architecture. As observed, E_k^{NL} increases monotonically with respect to $P_{\text{EH},k}$. Therefore, the minimum harvested power maximization problem in the non-linear power harvesting scenario is equivalent to

$$\underset{\{\mathbf{w}_k, \alpha_k, \mathbf{S}_0, \Gamma\}}{\text{maximize}} \quad \min_{k \in \mathcal{K}} P_{\text{EH},k} \tag{38a}$$

$$\text{s.t.} \quad \text{C1-C6}. \tag{38b}$$

Due to $\eta_k P_{\text{EH},k} = E_k$, the minimum harvested power maximization problem with non-linear power harvester has the same structure compared with that of linear power harvester. Hence, the proposed beamforming and reflecting optimization method in linear power harvesting scenario can be directly extended to the scenario with non-linear power harvesters.

IV. Robust Beamforming and Power Splitting Optimization With Imperfect CSI

The previous section investigates the problem of maximizing the minimum harvested power under the assumption of perfect CSI. In this section, we extend the analysis to a more

practical scenario where the CSI is imperfect. To this end, we define $\hat{\mathbf{H}}_k = [\text{diag}(\mathbf{h}_{r,k}^H)\mathbf{G}; \mathbf{h}_{d,k}^H]$, which can be decomposed into the estimated CSI and an estimation error term as

$$\hat{\mathbf{H}}_k = \hat{\mathbf{H}}_{\text{est},k} + \Delta\hat{\mathbf{H}}_k, \forall k \in \mathcal{K}, \tag{39}$$

where $\hat{\mathbf{H}}_{\text{est},k}$ denotes the estimated CSI, and $\Delta\hat{\mathbf{H}}_k$ represents the unknown estimation error. Following the approach in [62], we adopt a statistical model for the CSI error[8], given by

$$\begin{aligned} &\text{Vec}(\Delta\hat{\mathbf{H}}_k) \sim \mathcal{CN}(0, \mathbf{\Sigma}_k), \\ &\mathbf{\Sigma}_k \in \mathbb{C}^{(N+1)M\times(N+1)M} \succeq \mathbf{0}, \forall k \in \mathcal{K}. \end{aligned} \tag{40}$$

In contrast to the optimization problem formulated under perfect CSI (See Eq. (10)), the constraints that require modification in the presence of imperfect CSI are the minimum SINR constraint C2 and the power harvesting constraint (10b). Specifically, these are reformulated to account for the probabilistic nature of the CSI uncertainty:

$$\Pr\{\text{SINR}_k - \gamma_{\min,k} \geq 0\} \geq 1 - \rho_{I,k}, \forall k \in \mathcal{K}, \tag{41}$$

and

$$\Pr\{E_k - e \geq 0\} \geq 1 - \rho_{E,k}, \forall k \in \mathcal{K}, \tag{42}$$

where $\rho_{I,k} \in [0,1]$ and $\rho_{E,k} \in [0,1]$ represents the tolerable outage probability of SINR constraint and power harvesting constraints, respectively.

Lemma 3: (Bernstein-Type Inequality) Suppose $f(\mathbf{x}) = \mathbf{x}^H\mathbf{U}\mathbf{x} + 2\text{Re}(\mathbf{u}^H\mathbf{x}) + u$, where $\mathbf{U} \in \mathbb{C}^{n\times n} \succeq \mathbf{0}$, $\mathbf{u} \in \mathbb{C}^{n\times 1}$, $\mathbf{x} \in \mathbb{C}^{n\times 1} \sim \mathcal{CN}(0, \mathbf{I})$, and $u \in \mathbb{R}$. Then, for any $\rho \in [0,1]$, we have

$$\Pr\{f(\mathbf{x}) \geq 0\} \geq 1 - \rho \tag{43a}$$

$$\Rightarrow \begin{cases} \text{Tr}(\mathbf{U}) - \sqrt{2\ln(1/\rho)}a + \ln(\rho)b + u \geq 0 \\ \left\| \begin{matrix} \text{Vec}(\mathbf{U}) \\ \sqrt{2}\mathbf{u} \end{matrix} \right\|_2 \leq a \\ b\mathbf{I} + \mathbf{U} \succeq \mathbf{0},\ b \geq 0 \end{cases} \tag{43b}$$

where a and b are slack variables.

Based on *Lemma 3*, the probabilistic constraints (41)–(42) can be equivalently transformed into deterministic forms. Specifically, the probabilistic SINR constraint (41) is transformed into:

$$\begin{cases} \text{Tr}(\mathbf{U}_{I,k}) - \sqrt{2\ln(1/\rho_{I,k})}x_{I,k} + \ln(\rho_{I,k})y_{I,k} + u_{I,k} \geq 0, \\ \left\| \begin{matrix} \text{Vec}(\mathbf{U}_{I,k}) \\ \sqrt{2}\mathbf{u}_{I,k} \end{matrix} \right\|_2 \leq x_{I,k}, \\ y_{I,k}\mathbf{I} + \mathbf{U}_{I,k} \succeq \mathbf{0},\ y_{I,k} \geq 0, \end{cases} \tag{44}$$

where $x_{I,k}$ and $y_{I,k}$ are slack variables associated with the SINR constraint. Likewise, the power harvesting constraint (42) can be equivalently expressed as

$$\begin{cases} \text{Tr}(\mathbf{U}_{E,k}) - \sqrt{2\ln(1/\rho_{E,k})}x_{E,k} + \ln(\rho_{E,k})y_{E,k} + u_{E,k} \geq 0, \\ \left\| \begin{matrix} \text{Vec}(\mathbf{U}_{E,k}) \\ \sqrt{2}\mathbf{u}_{E,k} \end{matrix} \right\|_2 \leq x_{E,k}, \\ y_{E,k}\mathbf{I} + \mathbf{U}_{E,k} \succeq \mathbf{0},\ y_{E,k} \geq 0, \end{cases} \tag{45}$$

where $x_{E,k}$ and $y_{E,k}$ denote the slack variables correspond to the power harvesting constraint. Moreover, we define $\mathbf{W}_{\text{aux},k} = \frac{\mathbf{W}_k}{\gamma_{\min,k}} - \sum_{i=1,i\neq k}^{K}\mathbf{W}_i - \mathbf{S}_0$, $\mathbf{W}_{\text{tot}} = \mathbf{S}_0 + \sum_{i=1}^{K}\mathbf{W}_i$, $\mathbf{U}_{I,k} = \epsilon_u^2(\mathbf{W}_{\text{aux},k}^T \otimes \hat{\mathbf{V}})$, $\mathbf{u}_{I,k} = \epsilon_u\text{Vec}(\hat{\mathbf{V}}^H\hat{\mathbf{H}}_{\text{est},k}\mathbf{W}_{\text{aux},k}^H)$, $u_{I,k} = \text{Tr}(\mathbf{W}_{\text{aux},k}\hat{\mathbf{H}}_{\text{est},k}^H\hat{\mathbf{V}}\hat{\mathbf{H}}_{\text{est},k}) - \delta_k^2 - \frac{\zeta_k^2}{\alpha_k}$, $\mathbf{U}_{E,k} = \epsilon_u^2(\mathbf{W}_{\text{tot}}^T \otimes \hat{\mathbf{V}})$, $\mathbf{u}_{E,k} = \epsilon_u\text{Vec}(\hat{\mathbf{V}}^H\hat{\mathbf{H}}_{\text{est},k}\mathbf{W}_{\text{tot}}^H)$, $u_{E,k} = \text{Tr}(\mathbf{W}_{\text{tot}}\hat{\mathbf{H}}_{\text{est},k}^H\hat{\mathbf{V}}\hat{\mathbf{H}}_{\text{est},k}) + \delta_k^2 - \frac{e}{\eta_k(1-\alpha_k)}$, $\text{Vec}(\Delta\hat{\mathbf{H}}_k) = \epsilon_u\mathbf{i}_k$ with $\mathbf{i}_k \sim \mathcal{CN}(0, \mathbf{I}_{(N+1)M})$. By replacing constraint C2 and constraint (12) in the original optimization problem with their deterministic counterparts (44) and (45), respectively, we construct an alternating optimization framework to obtain a stationary solution to the minimum harvested power maximization problem under imperfect CSI. This framework proceeds by alternately solving the following three subproblems:

$$\underset{\substack{\{\mathbf{W}_k,\mathbf{S}_0,\\ x_{I,k},y_{I,k},\\ x_{E,k},y_{E,k},e\}}}{\text{maximize}} \quad e \tag{46a}$$

$$\text{s.t.} \quad \text{Tr}\left(\mathbf{A}(\phi_l)\left(\mathbf{S}_0 + \sum_{k=1}^{K}\mathbf{W}_k\right)\right) \geq b_{\min,l}, \forall l \in \mathcal{L}, \tag{46b}$$

$$\mathbf{S}_0 \succeq 0, \mathbf{W}_k \succeq 0, \forall k \in \mathcal{K}, \tag{46c}$$

$$\text{Tr}(\mathbf{S}_0) + \sum_{k=1}^{K}\text{Tr}(\mathbf{W}_k) \leq P_{\max,B}, \tag{46d}$$

$$\text{(44)-(45)}, \tag{46e}$$

$$\underset{\substack{\{\hat{\mathbf{V}},x_{I,k},y_{I,k},\\ x_{E,k},y_{E,k},e\}}}{\text{maximize}} \quad e \tag{47a}$$

$$\text{s.t.} \quad \hat{\mathbf{V}}_{n,n} = 1, \forall n \in \{\mathcal{N}, N+1\}, \tag{47b}$$

$$\text{(44)-(45)}, \tag{47c}$$

and

$$\underset{\{\alpha_k,e\}}{\text{maximize}} \quad e \tag{48a}$$

$$\text{s.t.} \quad \text{Tr}(\mathbf{U}_{I,k}) - \sqrt{2\ln(1/\rho_{I,k})}x_{I,k} + \ln(\rho_{I,k})y_{I,k} + u_{I,k} \geq 0, \forall k \in \mathcal{K}, \tag{48b}$$

$$\text{Tr}(\mathbf{U}_{E,k}) - \sqrt{2\ln(1/\rho_{E,k})}x_{E,k} + \ln(\rho_{E,k})y_{E,k} + u_{E,k} \geq 0, \forall k \in \mathcal{K} \tag{48c}$$

$$0 \leq \alpha_k \leq 1, \forall k \in \mathcal{K}. \tag{48d}$$

Based on optimization theory, problems (46)–(48) can be

[8]In general, channel error models can be categorized into two types, namely the bounded CSI error model and the statistical CSI error model. In this paper, we adopt the statistical CSI error model to characterize the channels between the BS and users, as the bounded CSI error model tends to be overly conservative. Moreover, the statistical CSI error model provides a more realistic representation of practical channel estimation errors, whereas the bounded CSI error model is typically employed to account for quantization-induced errors.

verified to be convex. Hence, standard convex solvers such as MOSEK can be employed to efficiently solve these subproblems in an alternating manner. The complete procedure is summarized in Algorithm 3, which outlines the proposed robust beamforming and power splitting strategy for the minimum harvested power maximization problem under imperfect CSI.

Algorithm 3: Robust beamforming and power splitting strategy for handling the minimum harvested power maximization problem under imperfect CSI

1 Set the iteration factor $n = 1$, outage probability thresholds $\{\rho_{I,k}, \rho_{E,k}\}$, and channel uncertainty factor ϵ_u. Initialize $\{\hat{\mathbf{V}}^{(0)}, \alpha_k^{(0)}\}$.
2 **Repeat:**
3 Given $\{\hat{\mathbf{V}}^{(n-1)}, \alpha_k^{(n-1)}\}$, calculate optimal $\{\mathbf{W}_k^{(n)}, \mathbf{S}_0^{(n)}\}$ by solving (46);
4 Given $\{\mathbf{W}_k^{(n)}, \mathbf{S}_0^{(n)}, \alpha_k^{(n-1)}\}$, acquire the optimal $\hat{\mathbf{V}}^{(n)}$ and auxiliary variables $\{x_{I,k}, x_{E,k}, y_{I,k}, y_{E,k}\}$ by solving (47) through penalty function-based method;
5 Given $\{\mathbf{W}_k^{(n)}, \mathbf{S}_0^{(n)}, \hat{\mathbf{V}}^{(n)}\}$ and auxiliary variables $\{x_{I,k}, x_{E,k}, y_{I,k}, y_{E,k}\}$, compute $\{\alpha_k^{(n)}\}$ by solving (48);
6 Update iteration factor $n = n + 1$;
7 **Until** convergence.
8 **Output:** optimal solution $(\mathbf{W}_k^*, \mathbf{S}_0^*, \hat{\mathbf{V}}^*, \alpha_k^*)$.

Finally, we analyze the convergence and computational complexity of Algorithm 3. According to the principle of the alternating optimization method, the objective value in each iteration satisfies the following inequality chain:

$$\begin{aligned} e(\mathbf{W}_k^{(n)}, \mathbf{S}_0^{(n)}, \hat{\mathbf{V}}^{(n)}, \alpha_k^{(n)}) &\overset{(\vartheta_1)}{\leq} e(\mathbf{W}_k^{(n+1)}, \mathbf{S}_0^{(n+1)}, \hat{\mathbf{V}}^{(n)}, \alpha_k^{(n)}) \\ &\overset{(\vartheta_2)}{\leq} e(\mathbf{W}_k^{(n+1)}, \mathbf{S}_0^{(n+1)}, \hat{\mathbf{V}}^{(n+1)}, \alpha_k^{(n)}) \\ &\overset{(\vartheta_3)}{\leq} e(\mathbf{W}_k^{(n+1)}, \mathbf{S}_0^{(n+1)}, \hat{\mathbf{V}}^{(n+1)}, \alpha_k^{(n+1)}), \end{aligned} \tag{49}$$

where (ϑ_1), (ϑ_2), and (ϑ_3) hold due to the optimal update of the transmit beamforming, IRS reflect matrix, and power splitting ratios in steps 3–5 of Algorithm 3. Accordingly, the objective value of the minimum harvested power maximization problem under imperfect CSI is non-decreasing across iterations. Furthermore, since the harvested power is inherently upper-bounded by a finite value, convergence to a stationary point is guaranteed after a finite number of iterations.

Defining I_3 as the iteration number of Algorithm 3, and ϵ_3, ϵ_4, and ϵ_5 as the accuracy tolerances for solving problems (46), (47), and (48), respectively. In Step 3, the optimal transmit beamforming is obtained by solving problem (46), which involves $(K+1)M^2 + 4K + 1$ variables and $L + 9K + 2$ constraints, resulting in a computational complexity of $\mathcal{O}(((K+1)M^2 + 13K + L + 3)((K+1)M^2 + 4K + 1)^2\sqrt{L+9K+2}\log(1/\epsilon_3))$. In Step 4, the optimal phase shift matrix is computed by solving problem (47), which includes $(N+1)^2 + 4K + 1$ variables and $8K + N + 1$ constraints. The associated complexity is given by $\mathcal{O}(((N+1)^2 + 12K + N + 2)((N+1)^2 + 4K + 1)^2\sqrt{8K+N+1}\log(1/\epsilon_4))$. In Step 5, the optimal power splitting ratios are obtained by solving problem (48), which involves $K+1$ variables and $4K$ constraints, with complexity $\mathcal{O}(2(5K+1)(K+1)^2\sqrt{K}\log(1/\epsilon_5))$. Hence, the overall computational complexity of Algorithm 3 is expressed as $\mathcal{O}(I_3(((K+1)M^2 + 13K + L + 3)((K+1)M^2 + 4K + 1)^2\sqrt{L+9K+2}\log(1/\epsilon_3) + ((N+1)^2 + 12K + N + 2)((N+1)^2 + 4K + 1)^2\sqrt{8K+N+1}\log(1/\epsilon_4) + 2(5K+1)(K+1)^2\sqrt{K}\log(1/\epsilon_5)))$.

V. Numerical Results

To evaluate the performance of the proposed joint transmit and reflect beamforming method, we compare it with the following benchmark schemes:

- *IRS with random phase:* The IRS phase shift is randomly generated following a uniform distribution over $[0, 2\pi]$, and remains fixed during the optimization. The remaining steps of the proposed algorithm, including the transmit beamforming and power splitting design, are retained and optimized based on the fixed IRS phase shift.
- *Without IRS:* In this baseline, the IRS is removed from the system. The BS performs radar sensing, information transmission, and power transfer solely via direct links to users/targets. The optimization involves only the transmit beamforming and power splitting ratios, based on a simplified version of the proposed algorithm.
- *Without radar sensing [58]:* The BS conducts downlink information and power transfer with IRS assistance. The transmit and reflect beamformers, along with the power splitting ratios, are jointly optimized to maximize the minimum harvested power across all users.
- *Sum harvested power maximization (SHPM)-based method [21]:* This scheme maximizes the total power harvested by all users, subject to the SINR requirements for information transmission and the beamforming gain constraints for radar sensing.
- *SDR-based Method:* The transmit beamforming and power splitting ratios are optimized using the proposed method. The phase shifts of the IRS are determined by solving problem (24) while relaxing the rank-one constraint[9].

In simulation experiments, we consider a scenario including multiple users and $L = 2$ sensing targets. The location of BS and IRS are set as [0,0,4] and [10,1,2], respectively. Users are randomly distributed within a square region of side length 5, centered at the horizontal coordinate [12.5, -2.5], with all users located on the $z = 0$ plane. In addition, the target sensing directions are set as $-\frac{\pi}{3}$ and $\frac{\pi}{3}$, respectively. The indoor propagation environment is modeled following the 3GPP TR 36.814 specifications [63]. The path loss is given by $10^{-(89.5+16.9\log_{10}(d))/10}$, where d represents the distance

[9]Due to the rank-one constraint is ignored in problem (24), the benchmark method 5 will provide an upper bound for original phase shift optimization subproblem (24).

between the transmitter and receiver. Besides, the transmit-receive antenna gain is set as 20 dBi. Furthermore, the small-scale fading is characterized by the Rician distribution with Rician factor being 3 [29]. Besides, we set the other simulation parameters as follows: the distance between two adjacent antennas at BS is set as $d = \frac{\lambda}{2}$, the linerar energy coversion efficiency is $\eta_k = 0.8$ [64], [65], the additive Gaussian noise power are set as $\delta_k^2 = 10^{-9}$ W and $\zeta_k^2 = 10^{-11}$ W, the penalty and tolerance factors of Algorithm 1 are set as $\nu = 10^{-11}$ and $\iota = 10^{-3}$, respectively, the channel uncertainty factor is $\epsilon_u = 10^{-5}$, the parameters associated with non-linear power harvesting model are $P_{\text{sat}} = 0.024$ W, $a = 150$, and $b = 0.014$ [48], [66].

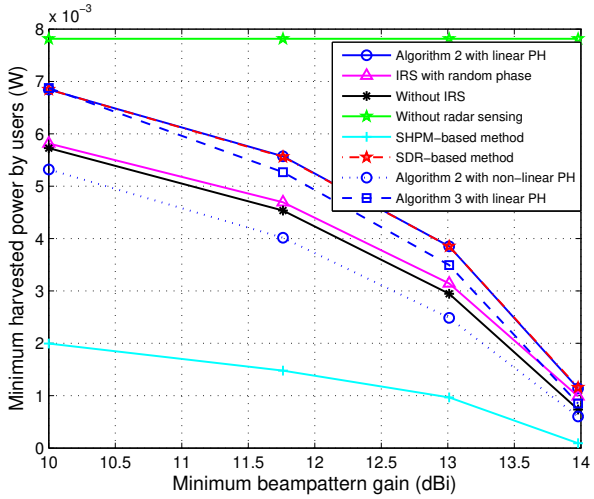

Fig. 3: Minimum beampattern gain versus minimum harvested power among all users.

In Fig. 3, we show the minimum beampattern gain $b_{\min,l}$ against the minimum harvested power among all users, where the minimum SINR requirement of users is set as $\gamma_{\min,k} = 8$ dB, the maximum transmit power of BS is $P_{\max,B} = 50$ W [27], and the number of BS antennas, IRS reflection elements and users are set as $M = 8$, $N = 30$ and $K = 4$, respectively. Among the schemes considered, excluding the benchmark method ignoring the radar sensing, the minimum harvested power achieved by the other schemes decreases as the minimum beampattern gain increases. This trend arises because the BS requires more power allocation for radar sensing when $b_{\min,l}$ is large, consequently reducing the available energy for power and information transmissions. Furthermore, we also find that the proposed method can realize significantly higher minimum harvested power of users compared with *IRS with random phase* scheme and *Without IRS* scheme, especially when the minimum beampattern gain $b_{\min,l}$ is small. That is due to the fact that the optimal IRS configuration can improve the composite channel gain between BS and users, and it will further lead to the increase of minimum power harvested by users. Another observation is that the proposed method outperforms *SHPM-based method*. This can be attributed to the fact that in *SHPM-based method*, the power harvested by the worst-case user is sacrificed to maximize the total power harvested by all users.

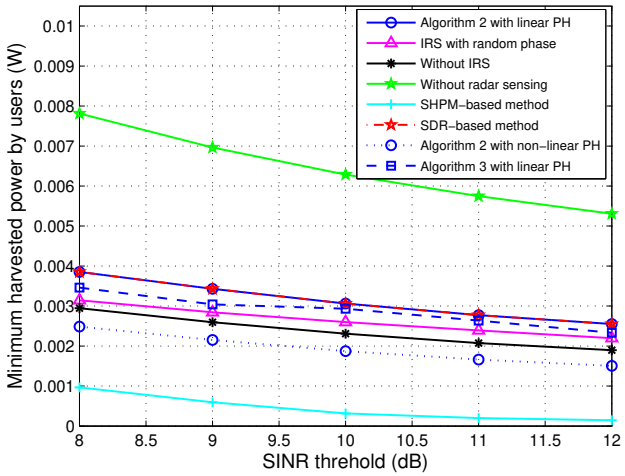

Fig. 4: SINR threshold versus minimum harvested power among all users.

Fig. 4 plots the SINR threshold against the minimum harvested power among all users, where $P_{\max,B} = 50$ W, $M = 8$, $N = 30$, $K = 4$, and the minimum beampattern gain for radar sensing is set as $b_{\min,l} = 13$ dBi. As observed, the minimum harvested power of users achieved by all the schemes decreases with the increase of SINR threshold. According to (5), the SINR of k-th user increases with its power splitting ratio α_k. Therefore, each user has to split a larger ratio of received signals to decode information when the SINR threshold is large. It will further reduce received signal ratios to harvest power at users. Furthermore, the proposed method achieves a significantly higher minimum harvested power among all users compared to *IRS with random phase* scheme, *Without IRS* scheme, and *SHPM-based method*. Meanwhile, this figure further demonstrates that the proposed approach employing a nonlinear power harvesting model yields lower harvested power relative to its linear counterpart. This discrepancy primarily stems from diminished rectification efficiency caused by nonlinear impedance characteristics at low input power levels, which exacerbates impedance mismatches and compromises energy conversion efficiency [67].

Fig. 5 reveals the relationship between the maximum transmit power of BS and the minimum harvested power among all users, where $\gamma_{\min,k} = 8$ dB, $b_{\min,l} = 10$ dBi, $M = 8$, $N = 30$, and $K = 4$. As observed, the minimum power harvested among all users tends to increase with the maximum transmit power of the BS. However, it's important to note that the power harvested by users cannot indefinitely increase with the maximum transmit power of the BS due to limitations imposed by the rectifying circuit. Furthermore, an interesting observation is that the performance gap between the proposed method and the *Without radar sensing* scheme widens inversely with the maximum transmit power of the BS. This phenomenon occurs because when $P_{\max,B}$ is large, the BS has sufficient power to simultaneously conduct radar sensing, information, and power transmissions. Consequently, the

This article has been accepted for publication in IEEE Internet of Things Journal. This is the author's version which has not been fully edited and content may change prior to final publication. Citation information: DOI 10.1109/JIOT.2025.3604835

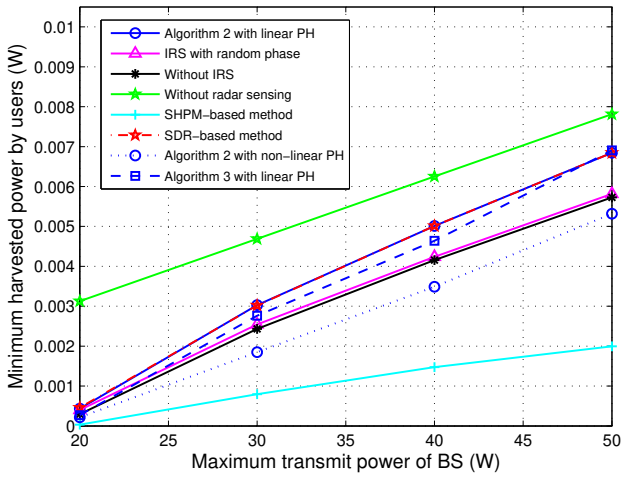

Fig. 5: Maximum transmit power of BS versus minimum harvested power among all users.

impact of radar sensing on the performance of information and power transmissions becomes negligible. Moreover, compared to the *IRS with random phase* scheme and the *Without IRS* scheme, the performance gain achieved by proposed method wides with the increase of maximum transmit power of BS. This observation highlights the importance of optimizing the IRS reflection parameters to enhance power transfer efficiency, particularly in scenarios when the maximum transmit power of AP is large enough. In addition, Figs. 3–5 illustrate that the proposed method under perfect CSI achieves slightly higher minimum harvested power across all users compared to the case with imperfect CSI. This observation confirms that channel estimation errors adversely affect the power transfer performance of the considered system.

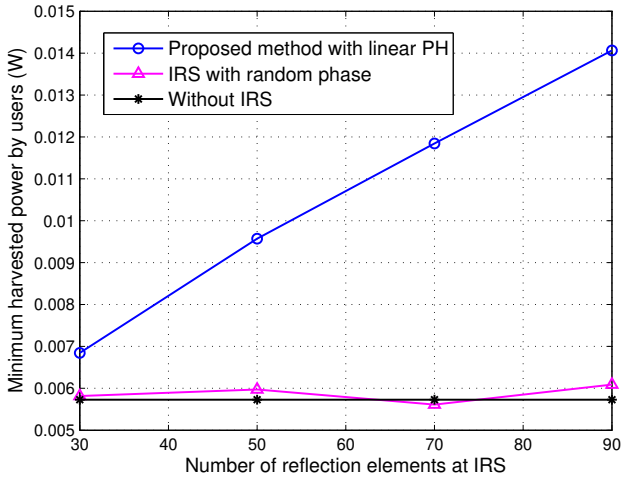

Fig. 6: Number of reflection elements versus minimum harvested power among all users.

Fig. 6 illustrates the relationship between the number of reflecting elements and the minimum harvested power across all users, where $P_{\max,B} = 50$ W, $\gamma_{\min,k} = 8$ dB, $b_{\min,l} = 10$ dBi, $M = 8$, and $K = 4$. The results demonstrate that the proposed method achieves a significantly higher minimum harvested power compared to both the *IRS with random phase* scheme and *Without IRS* scheme. Notably, the performance gap widens as the number of reflecting elements increases. Interestingly, the *IRS with random phase* scheme occasionally yields worse performance than the *Without IRS* scheme, when the number of reflection elements equals to 70. This is mainly due to the misalignment of reflected signals caused by improperly configured phase shifts, which can lead to destructive interference and degraded energy harvesting performance. These observations further highlight the importance of optimizing the IRS phase shifts to fully exploit the potential of IRS-assisted integrated sensing, communication, and powering systems.

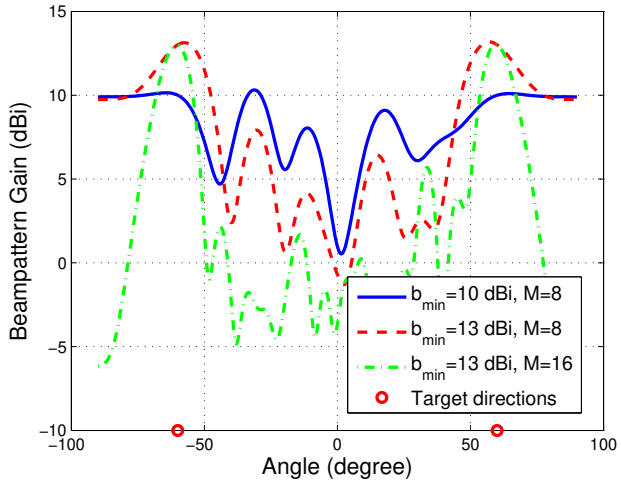

Fig. 7: Beampattern gain achieved by the proposed method.

Fig. 7 depicts the beampattern gain achieved by the proposed method, where $P_{\max,B} = 50$ W, $\gamma_{\min,k} = 8$ dB, $M = 8$, $N = 30$, and $K = 4$. As observed from this figure, the beampattern gains towards target angles realized by our proposed method are larger than $b_{\min,l}$, and it verifies that the proposed method can satisfy the multi-target sensing requirements. In addition, we find that the achievable sensing accuracy will be improved with the increase of M. Because the additional antennas installed at the BS will offer extra degrees of freedom to design the refined sensing beamforming. Moreover, it is also observed that the sensing performance is enhanced with the increase of $b_{\min,l}$. Because a larger $b_{\min,l}$ will impose the BS to design beamforming strategy for enhancing the sensing beampattern gains towards target directions.

Fig. 8 unveils the relationship between the number of users and the minimum harvested power among all users, where $P_{\max,B} = 60$ W, $\gamma_{\min,k} = 8$ dB, $b_{\min,l} = 10$ dBi, $M = 20$, and $N = 30$. As shown in the figure, the minimum harvested power across all users decreases as the number of users increases. This trend can be attributed to the limited capability of the BS to simultaneously satisfy the growing requirements of

This article has been accepted for publication in IEEE Internet of Things Journal. This is the author's version which has not been fully edited and content may change prior to final publication. Citation information: DOI 10.1109/JIOT.2025.3604835

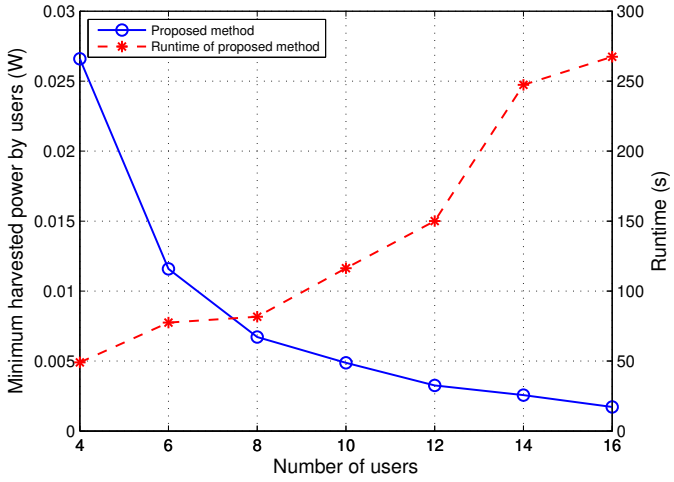

Fig. 8: Number of users versus minimum harvest power by users/runtime of proposed algorithm.

information transmission and power harvesting imposed by an increasing number of users. Meanwhile, it is observed that the runtime of the proposed algorithm increases with the number of users, primarily due to the growing problem dimensionality and iterative optimization overhead. These observations suggest promising opportunities for designing more efficient and scalable algorithms with reduced computational complexity, which can facilitate real-time implementation in large-scale IRS-assisted sensing, communication and powering systems[10].

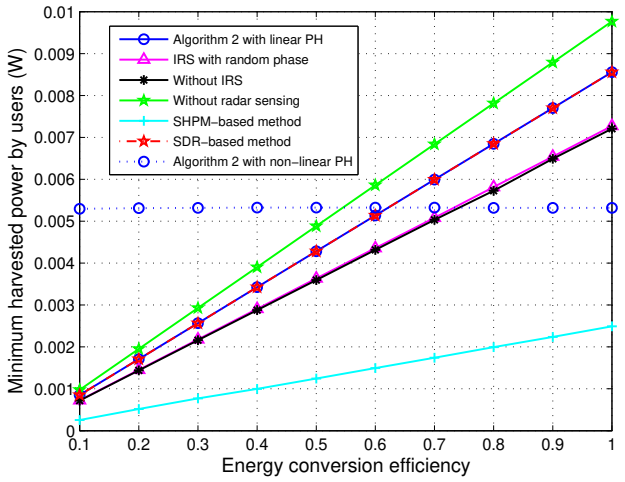

Fig. 9: Energy conversion efficiency versus minimum harvested power among all users.

Fig. 9 illustrates the relationship between the linear energy conversion efficiency and the minimum harvested power across all users, where $P_{\max,B} = 50$ W, $\gamma_{\min,k} = 8$ dB, $b_{\min,l} = 10$ dBi, $M = 8$, $N = 30$, and $K = 4$. It can be observed that, apart from the proposed method employing a non-linear power harvesting model, the minimum harvested power achieved by all the other schemes increases linearly with the energy conversion efficiency. Furthermore, the minimum harvested power typically ranges from 1 mW to 10 mW, which is sufficient to sustain a broad range of low-power IoT applications. Specifically, when the harvested power falls within 1-3 mW (corresponding to an energy conversion efficiency below 0.3), it is adequate to support ultra-low-power tasks such as ambient sensing (e.g., temperature and humidity monitoring) and intermittent radio frequency identification (RFID)-based communications [68]. As the harvested power increases to 3-6 mW (with energy conversion efficiency ranging from 0.3 to 0.7), more advanced functionalities become feasible, including wireless metering and bluetooth low energy (BLE)-based beacon broadcasting [69]. When the harvested power further rises to 6-8 mW (with energy conversion efficiency exceeding 0.7), the system is capable of supporting more frequent and energy-intensive operations, such as real-time equipment monitoring and periodic data transmission [70]. These findings demonstrate the potential of IRS-assisted sensing, communication, and powering systems to enable sustainable operation of distributed low-power IoT devices through efficient wireless energy transfer.

[10]It is worth noting that all simulations are coducted in MATLAB 2012 R2012a of MACBOOK Air. Besides, MOSEK is called to solve the formulated optimization problems.

VI. Conclusion

This article studied the optimal transmission and reflection method for IRS-enhanced integrated sensing, communication, and powering systems. We formulated a minimum harvested power maximization problem considering the target sensing and information transmission requirements. To address such a strictly non-convex problem, the BCD algorithm, SDR technique and penalty function-based method were adopted to iteratively optimize the transmit beamformer at the BS, reflect matrix of the IRS, and power splitting ratios of users. Moreover, we further proposed the robust beamforming and power splitting method for considered systems under imperfect CSI. Numerical results verified that our proposed method highly outperforms several existing benchmarks with regard to minimum harvested power among all users.

Additionally, this article opens avenues for exploration in several compelling research directions. Firstly, it is interesting to extend this work to the multiple-cell scenario, where inter-cell interference poses significant challenges. In such scenario, coordinate beamforming and scalable optimization will be essential to ensure reliable target sensing, information communication, and power transfer. Secondly, this work can be extended to scenarios with imperfect angle information, which would require the incorporation of angular uncertainty models and the application of stochastic constraint-based optimization techniques. Thirdly, the utilization of active IRS holds promise in mitigating the significant path attenuation associated with SWIPT. Finally, the accuracy of radar sensing is often compromised by environmental clutters. Therefore, investigating transmission and reflection optimization strategies focused on sensing accuracy for IRS-enhanced integrated sensing, communication, and powering systems in cluttered environments emerges as an essential research endeavor.

REFERENCES

[1] A. Liu, Z. Huang, M. Li, Y. Wan, W. Li, T. X. Han, C. Liu, R. Du, D. K. P. Tan, J. Lu, Y. Shen, F. Colone, and K. Chetty, "A survey on fundamental limits of integrated sensing and communication," *IEEE Communications Surveys and Tutorials*, vol. 24, no. 2, pp. 994–1034, 2022.

[2] K. Meng, Q. Wu, S. Ma, W. Chen, K. Wang, and J. Li, "Throughput maximization for UAV-enabled integrated periodic sensing and communication," *IEEE Transactions on Wireless Communications*, vol. 22, no. 1, pp. 671–687, 2023.

[3] C. Ouyang, Y. Liu, H. Yang, and N. Al-Dhahir, "Integrated sensing and communications: A mutual information-based framework," *IEEE Communications Magazine*, vol. 61, no. 5, pp. 26–32, 2023.

[4] M. Hua, Q. Wu, W. Chen, Z. Fei, H. C. So, and C. Yuen, "Intelligent reflecting surface-assisted localization: Performance analysis and algorithm design," *IEEE Wireless Communications Letters*, vol. 13, no. 1, pp. 84–88, 2024.

[5] X. Tong, Z. Zhang, J. Wang, C. Huang, and M. Debbah, "Joint multi-user communication and sensing exploiting both signal and environment sparsity," *IEEE Journal of Selected Topics in Signal Processing*, vol. 15, no. 6, pp. 1409–1422, 2021.

[6] Y. Chen, H. Hua, J. Xu, and D. W. K. Ng, "ISAC meets SWIPT: Multi-functional wireless systems integrating sensing, communication, and powering," *IEEE Transactions on Wireless Communications*, pp. 1–1, 2024.

[7] X. Gan, C. Huang, Z. Yang, X. Chen, J. He, Z. Zhang, C. Yuen, Y. L. Guan, and M. Debbah, "Coverage and rate analysis for integrated sensing and communication networks," *IEEE Journal on Selected Areas in Communications*, pp. 1–1, 2024.

[8] Z. Liu, S. Aditya, H. Li, and B. Clerckx, "Joint transmit and receive beamforming design in full-duplex integrated sensing and communications," *IEEE Journal on Selected Areas in Communications*, vol. 41, no. 9, pp. 2907–2919, 2023.

[9] T. D. Ponnimbaduge Perera, D. N. K. Jayakody, S. K. Sharma, S. Chatzinotas, and J. Li, "Simultaneous wireless information and power transfer (SWIPT): Recent advances and future challenges," *IEEE Communications Surveys and Tutorials*, vol. 20, no. 1, pp. 264–302, 2018.

[10] Q. Shi, L. Liu, W. Xu, and R. Zhang, "Joint transmit beamforming and receive power splitting for MISO SWIPT systems," *IEEE Transactions on Wireless Communications*, vol. 13, no. 6, pp. 3269–3280, 2014.

[11] Y. Huang, M. Liu, and Y. Liu, "Energy-efficient SWIPT in IoT distributed antenna systems," *IEEE Internet of Things Journal*, vol. 5, no. 4, pp. 2646–2656, 2018.

[12] Y. Xu, C. Shen, Z. Ding, X. Sun, S. Yan, G. Zhu, and Z. Zhong, "Joint beamforming and power-splitting control in downlink cooperative SWIPT NOMA systems," *IEEE Transactions on Signal Processing*, vol. 65, no. 18, pp. 4874–4886, 2017.

[13] K. Xiong, B. Wang, and K. J. R. Liu, "Rate-energy region of SWIPT for MIMO broadcasting under nonlinear energy harvesting model," *IEEE Transactions on Wireless Communications*, vol. 16, no. 8, pp. 5147–5161, 2017.

[14] H. Sun, F. Zhou, R. Q. Hu, and L. Hanzo, "Robust beamforming design in a NOMA cognitive radio network relying on SWIPT," *IEEE Journal on Selected Areas in Communications*, vol. 37, no. 1, pp. 142–155, 2019.

[15] J. An, C. Yuen, C. Xu, H. Li, D. W. K. Ng, M. Di Renzo, M. Debbah, and L. Hanzo, "Stacked intelligent metasurface-aided MIMO transceiver design," *IEEE Wireless Communications*, vol. 31, no. 4, pp. 123–131, 2024.

[16] Z. Lin, H. Niu, K. An, Y. Hu, D. Li, J. Wang, and N. Al-Dhahir, "Pain without gain: Destructive beamforming from a malicious RIS perspective in IoT networks," *IEEE Internet of Things Journal*, vol. 11, no. 5, pp. 7619–7629, 2024.

[17] J. An, C. Xu, D. W. K. Ng, G. C. Alexandropoulos, C. Huang, C. Yuen, and L. Hanzo, "Stacked intelligent metasurfaces for efficient holographic MIMO communications in 6G," *IEEE Journal on Selected Areas in Communications*, vol. 41, no. 8, pp. 2380–2396, 2023.

[18] T. Gong, P. Gavriilidis, R. Ji, C. Huang, G. C. Alexandropoulos, L. Wei, Z. Zhang, M. Debbah, H. V. Poor, and C. Yuen, "Holographic MIMO communications: Theoretical foundations, enabling technologies, and future directions," *IEEE Communications Surveys and Tutorials*, vol. 26, no. 1, pp. 196–257, 2024.

[19] E. Basar, G. C. Alexandropoulos, Y. Liu, Q. Wu, S. Jin, C. Yuen, O. A. Dobre, and R. Schober, "Reconfigurable intelligent surfaces for 6G: Emerging hardware architectures, applications, and open challenges," *IEEE Vehicular Technology Magazine*, vol. 19, no. 3, pp. 27–47, 2024.

[20] C. Pan, H. Ren, K. Wang, M. Elkashlan, A. Nallanathan, J. Wang, and L. Hanzo, "Intelligent reflecting surface aided MIMO broadcasting for simultaneous wireless information and power transfer," *IEEE Journal on Selected Areas in Communications*, vol. 38, no. 8, pp. 1719–1734, 2020.

[21] Q. Wu and R. Zhang, "Weighted sum power maximization for intelligent reflecting surface aided SWIPT," *IEEE Wireless Communications Letters*, vol. 9, no. 5, pp. 586–590, 2020.

[22] A. Khalili, S. Zargari, Q. Wu, D. W. K. Ng, and R. Zhang, "Multi-objective resource allocation for IRS-aided SWIPT," *IEEE Wireless Communications Letters*, vol. 10, no. 6, pp. 1324–1328, 2021.

[23] Y. Gao, Q. Wu, G. Zhang, W. Chen, D. W. K. Ng, and M. D. Renzo, "Beamforming optimization for active intelligent reflecting surface-aided SWIPT," *IEEE Transactions on Wireless Communications*, vol. 22, no. 1, pp. 362–378, 2023.

[24] H. Pang, M. Cui, G. Zhang, and Q. Wu, "Joint beamforming design and resource allocation for double-IRS-assisted RSMA SWIPT systems," *Computer Communications*, vol. 196, pp. 229–238, 2022.

[25] Q. Wu and R. Zhang, "Joint active and passive beamforming optimization for intelligent reflecting surface assisted SWIPT under QoS constraints," *IEEE Journal on Selected Areas in Communications*, vol. 38, no. 8, pp. 1735–1748, 2020.

[26] D. Xu, V. Jamali, X. Yu, D. W. K. Ng, and R. Schober, "Optimal resource allocation design for large IRS-assisted SWIPT systems: A scalable optimization framework," *IEEE Transactions on Communications*, vol. 70, no. 2, pp. 1423–1441, 2022.

[27] Y. Zhao, B. Clerckx, and Z. Feng, "IRS-aided SWIPT: Joint waveform, active and passive beamforming design under nonlinear harvester model," *IEEE Transactions on Communications*, vol. 70, no. 2, pp. 1345–1359, 2022.

[28] S. Zargari, A. Khalili, Q. Wu, M. Robat Mili, and D. W. K. Ng, "Max-min fair energy-efficient beamforming design for intelligent reflecting surface-aided SWIPT systems with non-linear energy harvesting model," *IEEE Transactions on Vehicular Technology*, vol. 70, no. 6, pp. 5848–5864, 2021.

[29] R. Zhang, K. Xiong, Y. Lu, P. Fan, D. W. K. Ng, and K. B. Letaief, "Energy efficiency maximization in RIS-assisted SWIPT networks with RSMA: A PPO-based approach," *IEEE Journal on Selected Areas in Communications*, vol. 41, no. 5, pp. 1413–1430, 2023.

[30] A. M. Elbir, K. V. Mishra, M. R. B. Shankar, and S. Chatzinotas, "The rise of intelligent reflecting surfaces in integrated sensing and communications paradigms," *IEEE Network*, pp. 1–8, 2022.

[31] X. Wang, Z. Fei, J. Huang, and H. Yu, "Joint waveform and discrete phase shift design for RIS-assisted integrated sensing and communication system under cramer-rao bound constraint," *IEEE Transactions on Vehicular Technology*, vol. 71, no. 1, pp. 1004–1009, 2022.

[32] S. P. Chepuri, N. Shlezinger, F. Liu, G. C. Alexandropoulos, S. Buzzi, and Y. C. Eldar, "Integrated sensing and communications with reconfigurable intelligent surfaces: From signal modeling to processing," *IEEE Signal Processing Magazine*, vol. 40, no. 6, pp. 41–62, 2023.

[33] G. C. Alexandropoulos, N. Shlezinger, I. Alamzadeh, M. F. Imani, H. Zhang, and Y. C. Eldar, "Hybrid reconfigurable intelligent metasurfaces: Enabling simultaneous tunable reflections and sensing for 6G wireless communications," *IEEE Vehicular Technology Magazine*, vol. 19, no. 1, pp. 75–84, 2024.

[34] M. Hua, Q. Wu, C. He, S. Ma, and W. Chen, "Joint active and passive beamforming design for IRS-aided radar-communication," *IEEE Transactions on Wireless Communications*, vol. 22, no. 4, pp. 2278–2294, 2023.

[35] N. Huang, T. Wang, Y. Wu, Q. Wu, and T. Q. S. Quek, "Integrated sensing and communication assisted mobile edge computing: An energy-efficient design via intelligent reflecting surface," *IEEE Wireless Communications Letters*, vol. 11, no. 10, pp. 2085–2089, 2022.

[36] Y. He, Y. Cai, H. Mao, and G. Yu, "RIS-assisted communication radar coexistence: Joint beamforming design and analysis," *IEEE Journal on Selected Areas in Communications*, vol. 40, no. 7, pp. 2131–2145, 2022.

[37] H. Luo, R. Liu, M. Li, Y. Liu, and Q. Liu, "Joint beamforming design for RIS-assisted integrated sensing and communication systems," *IEEE Transactions on Vehicular Technology*, vol. 71, no. 12, pp. 13 393–13 397, 2022.

[38] X. Liu, H. Zhang, K. Long, M. Zhou, Y. Li, and H. V. Poor, "Proximal policy optimization-based transmit beamforming and phase-shift design in an IRS-aided ISAC system for the THz band," *IEEE Journal on Selected Areas in Communications*, vol. 40, no. 7, pp. 2056–2069, 2022.

[39] H. Zhang, "Joint waveform and phase shift design for RIS-assisted integrated sensing and communication based on mutual information," *IEEE Communications Letters*, vol. 26, no. 10, pp. 2317–2321, 2022.

[40] M. Luan, B. Wang, Z. Chang, T. Hamalainen, and F. Hu, "Robust beamforming design for RIS-aided integrated sensing and communication system," *IEEE Transactions on Intelligent Transportation Systems*, vol. 24, no. 6, pp. 6227–6243, 2023.

[41] R. Liu, M. Li, Y. Liu, Q. Wu, and Q. Liu, "Joint transmit waveform and passive beamforming design for RIS-aided DFRC systems," *IEEE Journal of Selected Topics in Signal Processing*, vol. 16, no. 5, pp. 995–1010, 2022.

[42] T. Wei, L. Wu, K. V. Mishra, and M. R. Bhavani Shankar, "Multi-IRS-aided doppler-tolerant wideband DFRC system," *IEEE Transactions on Communications*, pp. 1–1, 2023.

[43] X. Song, J. Xu, F. Liu, T. X. Han, and Y. C. Eldar, "Intelligent reflecting surface enabled sensing: Cramer-rao bound optimization," *IEEE Transactions on Signal Processing*, vol. 71, pp. 2011–2026, 2023.

[44] Y. Zhang, J. Chen, C. Zhong, H. Peng, and W. Lu, "Active IRS-assisted integrated sensing and communication in C-RAN," *IEEE Wireless Communications Letters*, vol. 12, no. 3, pp. 411–415, 2023.

[45] J. Li, G. Zhou, T. Gong, and N. Liu, "Beamforming design for active IRS-aided MIMO integrated sensing and communication systems," *IEEE Wireless Communications Letters*, pp. 1–1, 2023.

[46] C. Wang, C.-C. Wang, Z. Li, D. W. K. Ng, K.-K. Wong, N. Al-Dhahir, and D. Niyato, "STAR-RIS-enabled secure dual-functional radar-communications: Joint waveform and reflective beamforming optimization," *IEEE Transactions on Information Forensics and Security*, vol. 18, pp. 4577–4592, 2023.

[47] X. Gan, C. Huang, Z. Yang, C. Zhong, X. Chen, Z. Zhang, Q. Guo, C. Yuen, and M. Debbah, "Bayesian learning for double-RIS aided ISAC systems with superimposed pilots and data," *IEEE Journal of Selected Topics in Signal Processing*, pp. 1–16, 2024.

[48] H. Hua, J. Xu, and T. X. Han, "Optimal transmit beamforming for integrated sensing and communication," *IEEE Transactions on Vehicular Technology*, vol. 72, no. 8, pp. 10 588–10 603, 2023.

[49] B. Zheng, C. You, W. Mei, and R. Zhang, "A survey on channel estimation and practical passive beamforming design for intelligent reflecting surface aided wireless communications," *IEEE Communications Surveys and Tutorials*, vol. 24, no. 2, pp. 1035–1071, 2022.

[50] C. Liao, F. Wang, and V. K. N. Lau, "Optimized design for irs-assisted integrated sensing and communication systems in clutter environments," *IEEE Transactions on Communications*, vol. 71, no. 8, pp. 4721–4734, 2023.

[51] G. Cui, H. Li, and M. Rangaswamy, "MIMO radar waveform design with constant modulus and similarity constraints," *IEEE Transactions on Signal Processing*, vol. 62, no. 2, pp. 343–353, 2013.

[52] F. Liu, W. Yuan, C. Masouros, and J. Yuan, "Radar-assisted predictive beamforming for vehicular links: Communication served by sensing," *IEEE Transactions on Wireless Communications*, vol. 19, no. 11, pp. 7704–7719, 2020.

[53] C. Liang, J. Kuang, F. Wu, and J. Chen, "Millimetre-wave beam tracking: An intelligent machine learning and kalman filter fusion technology," *IEEE Transactions on Cognitive Communications and Networking*, vol. 10, no. 2, pp. 487–498, 2024.

[54] F. Liu, Y. Cui, C. Masouros, J. Xu, T. X. Han, Y. C. Eldar, and S. Buzzi, "Integrated sensing and communications: Toward dual-functional wireless networks for 6G and beyond," *IEEE Journal on Selected Areas in Communications*, vol. 40, no. 6, pp. 1728–1767, 2022.

[55] A. Beck and L. Tetruashvili, "On the convergence of block coordinate descent type methods," *SIAM journal on Optimization*, vol. 23, no. 4, pp. 2037–2060, 2013.

[56] Z.-Q. Luo, W.-K. Ma, A. M.-C. So, Y. Ye, and S. Zhang, "Semidefinite relaxation of quadratic optimization problems," *IEEE Signal Processing Magazine*, vol. 27, no. 3, pp. 20–34, 2010.

[57] M. Grant and S. Boyd, "CVX: Matlab software for disciplined convex programming, version 2.1," 2014.

[58] Y. Tang, G. Ma, H. Xie, J. Xu, and X. Han, "Joint transmit and reflective beamforming design for IRS-assisted multiuser MISO SWIPT systems," in *ICC 2020 - 2020 IEEE International Conference on Communications (ICC)*, 2020, pp. 1–6.

[59] X. Yu, D. Xu, Y. Sun, D. W. K. Ng, and R. Schober, "Robust and secure wireless communications via intelligent reflecting surfaces," *IEEE Journal on Selected Areas in Communications*, vol. 38, no. 11, pp. 2637–2652, 2020.

[60] J. Liao, M. R. Khandaker, and K.-K. Wong, "Robust power-splitting SWIPT beamforming for broadcast channels," *IEEE Communications Letters*, vol. 20, no. 1, pp. 181–184, 2015.

[61] Y. Shi, H. D. Tuan, H. Tuy, and S. Su, "Global optimization for optimal power flow over transmission networks," *Journal of Global Optimization*, vol. 69, pp. 745–760, 2017.

[62] S. Hong, C. Pan, H. Ren, K. Wang, K. K. Chai, and A. Nallanathan, "Robust transmission design for intelligent reflecting surface-aided secure communication systems with imperfect cascaded CSI," *IEEE Transactions on Wireless Communications*, vol. 20, no. 4, pp. 2487–2501, 2020.

[63] *Technical Specification Group Radio Access Network: Evolved Universal Terrestrial Radio Access (E-UTRA): Further Advancements for E-UTRA Physical Layer Aspects*, Tr 36.814 ed., 3GPP, Mar. 2017.

[64] H. Sadia, A. Kamal Hassan, Z. Haq Abbas, G. Abbas, T. Baker, and N. Saeed, "Maximizing energy efficiency in IRS-assisted phase cooperative PS-SWIPT-based self-sustainable iot network," *IEEE Open Journal of the Communications Society*, vol. 6, pp. 4311–4327, 2025.

[65] Z. Li, W. Chen, Q. Wu, K. Wang, and J. Li, "Joint beamforming design and power splitting optimization in irs-assisted SWIPT NOMA networks," *IEEE Transactions on Wireless Communications*, vol. 21, no. 3, pp. 2019–2033, 2022.

[66] E. Boshkovska, D. W. K. Ng, N. Zlatanov, and R. Schober, "Practical non-linear energy harvesting model and resource allocation for SWIPT systems," *IEEE Communications Letters*, vol. 19, no. 12, pp. 2082–2085, 2015.

[67] M. Babaei, L. Durak-Ata, and Ü. Aygölü, "New practical nonlinear energy-harvesting models for wireless-powered communications," *Wireless Communications and Mobile Computing*, vol. 2022, no. 1, p. 6534754, 2022.

[68] M. K. Mishu, M. Rokonuzzaman, J. Pasupuleti, M. Shakeri, K. S. Rahman, F. A. Hamid, S. K. Tiong, and N. Amin, "Prospective efficient ambient energy harvesting sources for IoT-equipped sensor applications," *Electronics*, vol. 9, no. 9, 2020. [Online]. Available: https://www.mdpi.com/2079-9292/9/9/1345

[69] Q. Liu, W. IJntema, A. Drif, P. Pawełczak, and M. Zuniga, "BEH: Indoor batteryless BLE beacons using rf energy harvesting for internet of things," 2019. [Online]. Available: https://arxiv.org/abs/1911.03381

[70] N. Garg and R. Garg, "Energy harvesting in IoT devices: A survey," in *2017 International Conference on Intelligent Sustainable Systems (ICISS)*, 2017, pp. 127–131.